# NATIONAL ADVISORY COMMITTEE FOR AERONAUTICS

TECHNICAL NOTE 4026

## EFFECTS OF THERMAL RELAXATION AND SPECIFIC-HEAT CHANGES ON MEASUREMENTS WITH A PNEUMATIC-PROBE PYROMETER

By P. W. Kuhns

Lewis Flight Propulsion Laboratory
Cleveland, Ohio


Washington
July 1957

Page

NATIONAL ADVISORY COMMITTEE FOR AERONAUTICS

TECHNICAL NOTE 4026

# EFFECTS OF THERMAL RELAXATION AND SPECIFIC-HEAT CHANGES ON MEASUREMENTS WITH A PNEUMATIC-PROBE PYROMETER

By P. W. Kuhns

## SUMMARY

Equations are derived which evaluate the effects of thermal vibrational relaxation and specific-heat changes on pneumatic-probe pyrometer measurements in the region 1000° to 3000° K and 0.3 < Mach number < 2.0. Examples are given for typical probes in two combustion mixtures.

## INTRODUCTION

During recent years much interest has been shown in the problem of the effects of thermal relaxation or disequilibrium of vibrational modes of excitation on various aerodynamic processes. The effect of the vibrational relaxation time on the thickness of shock waves has been investigated in reference 1, and the shock-wave thickness has been used to measure relaxation times in references 2 to 4. The effect of vibrational relaxation time on flow through a rocket nozzle is studied in reference 5. The manner in which vibrational relaxation affects the measurement of total pressure has been used to find the vibrational relaxation times of some gases in references 6 to 9. A discussion of the effects of relaxation on some nozzle processes is found in reference 10.

A review of vibrational relaxation measurements is presented in reference 11 with a fairly complete bibliography. This report also contains a table of room temperature values of the average number of collisions necessary to achieve vibrational relaxation as found by many investigators. Since that time (1951), work has been done both theoretically (refs. 12 to 14) and experimentally (refs. 2, 3, 4, 8, 9, 15, 16, and 17) in the determination of vibrational relaxation times. A more recent review of relaxation phenomena and their measurement may be found in reference 18.

This report considers the problem of the effects of vibrational relaxation on pneumatic-probe temperature measurements. The pneumatic-probe pyrometer does not directly measure the gas temperature but measures

other aerodynamic quantities and relates them to the gas temperature by means of theoretical equations. The basic formulation of the method may be found in references 19 to 23. Some experimental results using the method are reported in reference 21. Reference 23 presents data comparing the results of the method with simultaneous data from thermocouple and sodium D line reversal measurements.

As the gas flows from the free stream into the pyrometer, it suffers a partial stagnation because of the presence of the probe body and an acceleration because of the pressure drop in the probe. The result is a rapid change in the available thermal energy. The relaxation (response) times of some vibrational modes of thermal excitation are such that the modes cannot follow these changes. As a result, the critical velocity in the probe and the temperature as calculated are affected.

Equations are derived herein which can be used to correct the measured parameters in such a way as to obtain the proper temperature when the vibrational modes of a molecular species are only partially relaxed. By using these equations, the effects of thermal relaxation and specific-heat changes on the measured total pressure, the calculated total temperature, the critical velocity, and the mass-flow rate are considered. The equations are evolved in a general form so that they may be applicable to similar flow problems.

## THEORY

### Outline of Subscripts and Superscripts Used

As an aid in reading the text, the following guide to the subscripts and superscripts is presented. A complete list of symbols is presented in appendix A.

Subscripts. - The magnitude of many of the quantities used is dependent upon the state of relaxation or equilibrium of the modes of thermal excitation. For convenience it is possible to group the modes of thermal excitation of all the different molecules in a gas according to their probable state of thermal equilibrium or disequilibrium at the first nozzle of the pneumatic probe (fig. 1).

The first subscript denotes the relaxation group into which the quantity is to be placed.

| | |
|---|---|
| none | all modes |
| P | relaxed modes |

There are extremes in the quantities grouped as relaxed modes. These extremes occur when the partially relaxed vibrational mode approaches either full relaxation or an unrelaxed state. These extremes are denoted by:

R relaxed modes when partially relaxed mode is assumed relaxed

U relaxed modes when partially relaxed mode is assumed unrelaxed or "frozen"

Z relaxed modes when partially relaxed mode is assumed unrelaxed and specific heats of all modes are assumed to be independent of temperature

The other modes are designated as follows:

B partially relaxed vibrational modes

X vibrational modes which are considered unrelaxed or frozen

Thus,

$$E = E_P + E_B + E_X$$

A second subscript denoting the station where the quantity is to be taken is shown as 0, 1, 2, 3, or 4.

Superscripts. - Usually the state of relaxation also denotes the temperature at which a quantity is considered. When there are exceptions, the temperature state at which the quantity is to be taken is given by a superscript.

Thus, $E_B$ is the energy of the B mode taken at the temperature of the B mode, while $E_B^P$ is the energy of the B mode taken at the temperature of the P modes.

There is also a difference between the measured quantities and the quantities involved in the theoretical equations. The measured quantities will be designated by the superscript $^*$.

## Theory of Operation

In the pneumatic-probe method of gas temperature measurement, the total temperature is usually found by using the following procedure, with reference to figure 1:

(1) A pressure drop through the nozzles is established by an exhaust system large enough that the flow through both nozzles becomes critical. The mass flow reaches a maximum value (ref. 23).

(2) After passing through the first nozzle, the hot gas is cooled before reaching a second nozzle.

(3) The total pressure $P_4^*$ and the total temperature $T_4^*$ at the second nozzle are measured.

(4) The flow in the probe is halted and the total pressure $P_2^*$ is measured at the first nozzle using the probe as a pitot tube.

(5) The true total temperature $T_0$ of the gas is obtained as a function of the above measurements from aerodynamic relations equating the mass flows through the two nozzles.

## Velocity Profiles, Relaxation Times, and Specific-Heat Changes

In making the measurements outlined in the preceding section the gas flow is changed somewhat. Such changes in gas flow can, under some circumstances, affect the measurements.

As the gas passes from the free stream into the probe, it is first slowed down by the presence of the probe and then speeded up by the pressure drop at the nozzle. This is shown in figure 2, which presents measured velocity profiles below a free-stream Mach number $M_1 = 1$ for the center streamline of a simulated probe and shows the probe shape drawn to scale.

The inequality in the decelerating and accelerating distances (and, thus, times) should be noted in figure 2. For the typical probe size ($D \approx 1/2$ in.; $d \approx 1/8$ in.) in a gas at 2500° K with a free-stream Mach number near 1, the decelerating time is about 10 microseconds; the accelerating time is about 1 microsecond.

If the components of a gas are to remain in equilibrium during this process, energy must be exchanged between molecules and between modes of thermal excitation of the molecules. If this exchange takes longer than the accelerating time, the gas will not be in complete equilibrium, and the flow through the nozzle will be affected.

When the pressure $P_2^*$ is being measured, the flow through the nozzle is stopped. The velocity profile now is like that shown in figure 2 for the velocity ratio $u_2/u_1 = 0$. If the time a gas molecule

takes to stop in front of the probe is on the same order of magnitude as the time to reach equilibrium, the measured pressure $P_2^*$ will be affected.

At the temperatures, pressures, and velocities to which the probes are usually subjected, the rotational and translational modes of thermal excitation establish equilibrium in less than 1/10 microsecond so that they can follow the energy changes. However, some vibrational modes cannot follow the changes, having relaxation times $\tau$ of 0.1 to 10,000 microseconds.

The effect of this relaxation time upon temperature is shown in figure 3, in which a gas mixture is assumed that, at the first nozzle, has in its constituents one of three vibrational modes: one that is relaxed (in equilibrium), a vibrational mode that is unrelaxed (unaffected), and one that is partially relaxed. The temperature and velocity at the second nozzle are usually so low that any effects due to relaxation may be neglected.

It should be noted in figure 3 that not only does the relaxation of a vibrational mode affect the temperature of that mode, but, because energy must be conserved, it affects the temperatures of all relaxed modes.

The time to reach equilibrium is measured by the relaxation time, which is defined by the equation (refs. 11 and 18):

$$\frac{d}{dt}\theta_B = -\frac{1}{\tau}(\theta_B - \theta_P) \tag{1}$$

for constant vibrational specific heats.

To write equation (1) it was assumed that the specific heats were constant during the energy change. However, by using a very rough calculation it is easily seen that even at subsonic speeds the temperature of the gas may vary as much as 20 percent when the gas passes from the free stream into the probe. In the temperature range from 500° to 3000° K the vibrational specific heat of most gases will change with temperature. This is shown in table I which lists values obtained from reference 24. For this reason equation (1) should be modified to:

$$\frac{d}{dt}E_B = -\frac{1}{\tau}(E_B - E_B^P) \tag{2}$$

where $E_B^P$ is the energy of the partially relaxed vibrational mode taken at the temperature of the relaxed modes.

## Derivation of Equations for $T_0$

The true total temperature $T_0$ is defined as the temperature the gas would have if it were brought adiabatically to a stop with all modes in equilibrium:

$$T_0 \equiv \theta_0 = \frac{E_1 + \frac{u_1^2}{2}}{\frac{1}{\theta_0}\int dE} \tag{3}$$

This is the temperature which the probe is presumed to measure.

As an aid in calculation, a second temperature will be defined:

$$T_{Z,1} \equiv \theta_1 + \frac{u_1^2}{2c_{P,1}} = \theta_1\left(1 + \frac{\gamma_{P,1} - 1}{2} M_{Z,1}^2\right) \tag{4}$$

where

$$M_{Z,1}^2 = M_1^2 \frac{\gamma_1}{\gamma_{P,1}}$$

and $T_{Z,1}$ is not the total temperature but in many cases is close to it.

In the derivation of the relation between $T_0$ and the measured quantities $P_2^*$, $P_4^*$, and $T_4^*$, use is made of five fundamental equations which must be satisfied.

(1) The equation of conservation of energy:

$$E_B + E_P + E_{X,1} + \frac{u^2}{2} = E_{B,1} + E_{P,1} + E_{X,1} + \frac{u_1^2}{2} = c_{P,1}T_{Z,1} + E_{B,1} + E_{X,1} \tag{5}$$

(2) The equation for critical flow:

$$\frac{dm_2}{dp_2} = 0 = \frac{dm_4}{dp_4} \tag{6}$$

(3) The equation for entropy change:

$$\Delta S = \int dE_B \left(\frac{1}{\theta_B} - \frac{1}{\theta_P}\right) \tag{7}$$

(4) The relaxation equation (eq. (2))

(5) The equation for conservation of mass:

$$m_4 = m_2 = A_2\rho_2 u_2 = A_4\rho_4 u_4 \tag{8}$$

In order to find a usable solution to these equations, four assumptions are made:

(1) The specific heats vary linearly in the form

$$c_i = c_{i,1} + 2c_{i,1}\psi_i\left(\frac{\theta_i - \theta_1}{\theta_i}\right) \tag{9}$$

where $\psi_i$ is a constant and $i$ signifies any particular mode.

(2) The static pressure at station 2 is related to that at station 1 by the function

$$\frac{p_2}{p_1} = \left(\frac{\theta_{P,2}}{\theta_1}\right)^{\frac{n}{n-1}} \tag{10}$$

(3) The relaxation time $\tau$ is constant over the process in front of the nozzle.

(4) At station 1 all modes are in thermal equilibrium:

$$\theta_1 = \theta_{P,1} = \theta_{B,1} = \theta_{X,1} \tag{11}$$

By using the previous five basic equations and the four assumptions, an equation for $T_0$ is found:

$$T_0 = \left(\frac{A_2P_2^*}{A_4P_4^*}\right)^2 T_4^* \frac{h(\gamma_{P,1})}{h(\gamma_4)}(1 + \varepsilon_a)(1 + \varepsilon_b)(1 + \varepsilon_c) \tag{12}$$

where

$$h(\gamma) = \gamma\left(\frac{2}{\gamma + 1}\right)^{\frac{\gamma+1}{\gamma-1}} \tag{13}$$

and

$1 + \varepsilon_a$ correction to mass-flow rate due to relaxation and specific-heat change with gas passing through a nozzle

$1 + \varepsilon_b$ correction to total pressure due to relaxation and specific-heat change when the flow through the nozzle is stopped and $P_2$ is measured

$1 + \varepsilon_c$ $T_0/T_{Z,1}$

Appendix B gives a detailed derivation of the equations for $1 + \varepsilon_a$ and $1 + \varepsilon_b$. In part of appendix B the additional assumption is made that the equation for critical flow (eq. (6)) for the first nozzle is satisfied by a critical velocity given as

$$\left(\frac{u_2}{u_1}\right)^2 = \left(\frac{u_{Z,2}}{u_1}\right)^2 = (T_{Z,1})\left(\frac{2}{\gamma_{P,1} + 1}\right)\left(\frac{1}{M_{Z,1}}\right)^2 \tag{14}$$

Working Approximation of $1 + \varepsilon_a$, $1 + \varepsilon_b$, and $1 + \varepsilon_c$

Even when making an assumption as to the velocity (eq. (14)), the computation of $1 + \varepsilon_a$ and $1 + \varepsilon_b$ by these methods is still too complex to be of any use to the engineer. A working approximation was found that appears adequately accurate.

When computing $\varepsilon_a$ and $\varepsilon_b$ from the relaxation equations, the variables $\Sigma_a$, $\Sigma_b$, $\Gamma_a$, and $\Gamma_b$ appear. These variables are derived in appendix B and are given by

$$\Sigma_a \quad \text{or} \quad \Sigma_b = \int_0^{t_f} \left[\frac{d(u/u_1)^2}{dt}\right] e^{-(t_f - t)/\tau^+} \, dt \tag{15}$$

$$\frac{1}{2}\Gamma_a \quad \text{or} \quad \left(\frac{\theta_1}{\theta_{R,2}}\right)^2 \Gamma_b = \frac{1}{\tau^+}\int_0^{t_f} \left(\frac{\Sigma(t)}{\theta_R/\theta_1}\right)^2 dt \tag{16}$$

The velocity profile $u/u_1$ used to calculate $\Sigma_a$ and $\Gamma_a$ is that with flow through the nozzle. The velocity profile used to calculate $\Sigma_b$ and $\Gamma_b$ is that with the flow in the nozzle stopped.

With assumed values for $\theta_1$ and $M_{Z,1}$ the specific heats and values of $\psi$ are computed from tabulated data (ref. 24) or from tables I and II. The value of $u_2/u_1$ is computed from equation (13). Then $\varepsilon_a$ is calculated from the formula:

$$\varepsilon_a \approx \varepsilon_{a,U} + \left[1 - \frac{\Sigma_a}{(u_2/u_1)^2 - 1}\right](\varepsilon_{a,R} - \varepsilon_{a,U}) - \left(\frac{\gamma - 1}{2} M_1^2\right)^2 \frac{c_1 c_{B,1} \Gamma_a}{R c_{P,1}} \tag{17}$$

where $\varepsilon_{a,U}$ and $\varepsilon_{a,R}$ are the two extremes of $\varepsilon_a$, and $\Sigma_a$ is computed from the velocity profiles (eq. (14)). The functions $\varepsilon_{a,R}$ and $\varepsilon_{a,U}$ can be calculated from the following equations:

$$\varepsilon_{a,U} = \left(\frac{\theta_{U,2}}{\theta_{Z,2}}\right)^{\frac{2}{\gamma_{P,1}-1}} \left(\frac{\theta_{U,2}}{\theta_1}\right)^{2\beta_U} - 1 \tag{18}$$

where

$$\theta_{Z,2} = 2\theta_1 \frac{1 + \frac{\gamma_{P,1} - 1}{2} M_{Z,1}^2}{\gamma_{P,1} + 1} \tag{19}$$

$$R\beta_U \approx c_{P,1}\psi_P \left(\frac{\theta_{Z,2}}{\theta_1} - 1\right) \tag{20}$$

$$\theta_{U,2} = \theta_1 \frac{c_{P,1}\left(\frac{\theta_{Z,2}}{\theta_1} - 1\right)}{c_{P,1} + R\beta_U} + \theta_1 \tag{21}$$

$$\varepsilon_{a,R} = \left(\frac{\theta_{R,2}}{\theta_{Z,2}}\right)^{\frac{2}{\gamma_{P,1}-1}} \left(\frac{\theta_{R,2}}{\theta_1}\right)^{2\beta_R} - 1 \tag{22}$$

where

$$R\beta_R \approx c_{B,1} + (c_{P,1}\psi_P + c_{B,1}\psi_B)\left(\frac{\theta_{Z,2}}{\theta_1} - 1\right) \frac{c_{P,1}}{c_{P,1} + c_{B,1}} \tag{23}$$

$$\theta_{R,2} = \theta_1 \frac{c_{P,1}\left(\frac{\theta_{Z,2}}{\theta_1} - 1\right)}{c_{P,1} + R\beta_R} + \theta_1 \tag{24}$$

The curve for $\varepsilon_b$ is given by

$$\varepsilon_b = \varepsilon_{b,U} + (1 - \Sigma_b^2 - \Gamma_b)(\varepsilon_{b,R} - \varepsilon_{b,U}) \tag{25}$$

and

$$\varepsilon_{b,U} = \left(\frac{T_{Z,1}}{T_{U,2}}\right)^{\frac{2c_{P,1}}{R}} \left(\frac{\theta_1}{T_{U,2}}\right)^{2\beta_U^*} - 1 \tag{26}$$

where

$$T_{Z,1} = \theta_1\left(1 + \frac{\gamma_{P,1} - 1}{2} M_{Z,1}^2\right) \tag{27}$$

$$R\beta_U^* \approx c_{P,1}\psi_P\left(\frac{T_{Z,1}}{\theta_1} - 1\right) \tag{28}$$

$$T_{U,2} = \theta_1 \frac{c_{P,1}\left(\frac{T_{Z,1}}{\theta_1} - 1\right)}{c_{P,1} + R\beta_U^*} + \theta_1 \tag{29}$$

and

$$\varepsilon_{b,R} = \left(\frac{T_{Z,1}}{T_{R,2}}\right)^{\frac{2c_{P,1}}{R}} \left(\frac{\theta_1}{T_{R,2}}\right)^{2\beta_R^*} - 1 \tag{30}$$

where

$$R\beta_R^* = c_{B,1} + (c_{P,1}\psi_P + c_{B,1}\psi_B)\left(\frac{T_{Z,1}}{\theta_1} - 1\right)\left(\frac{c_{P,1}}{c_{B,1} + c_{P,1}}\right) \tag{31}$$

$$T_{R,2} = \theta_1 \frac{c_{P,1}\left(\frac{T_{Z,1}}{\theta_1} - 1\right)}{c_{P,1} + R\beta_R^*} + \theta_1 \tag{32}$$

By using the assumption expressed in equation (9), a relation for $1 + \varepsilon_c$ may be written in the following manner:

$$1 + \varepsilon_c \approx \frac{c_{P,1}\left(1 - \frac{\theta_1}{T_{Z,1}}\right)}{c_1 + c_1\psi\left(\frac{T_{Z,1}}{\theta_1} - 1\right)\frac{c_{P,1}}{c_1}} + \frac{\theta_1}{T_{Z,1}} \tag{33}$$

By using the above equations comparisons were made with the more complex formulas outlined in appendix B. The above equations are shown in appendix B to be accurate in the region $0.3 < M_1 < 1.4$. Modifications of the above formulas for the region $1.4 < M_1 < 2.0$ are given in appendix B (eq. (B58)). Below $M_1 = 0.3$, $u_2/u_1$ cannot be assumed constant.

## Other Corrections

Specific-heat ratio. - If in the computation of $h(\gamma_{P,1})/h(\gamma_4)$ some other value of $\gamma$ was used instead of $\gamma_{P,1}$, a correction can be made of

$$1 + \varepsilon_d \approx \frac{h(\gamma_{P,1})}{h(\gamma)} \tag{34}$$

Discharge coefficient. - In all the previous derivations the effective areas A were used. These areas are equal to the discharge coefficient multiplied by $\pi d^2/4$. The discharge coefficient is affected by thermal relaxation. By using reference 23, an estimate of the error induced by neglecting this change was calculated. The maximum error varied from 0.04 percent at $M_1 = 0$ to -0.2 percent at $M_1 = 2.0$. Thus, this effect may be neglected over the range of velocities and temperatures considered in this report.

Dissociation. - In all the previous derivations and equations it has been assumed that the specific gas constant R was the same at both nozzles. Above 2000° K, dissociation of the gas products of combustion

make this assumption false. If differences in R are allowed, equation (12) should be rewritten as

$$T_0 = \left(\frac{A_2 P_2^*}{A_4 P_4^*}\right)^2 T_4^* \left[\frac{h(\gamma_{P,1})}{h(\gamma_4)}\right] (1 + \varepsilon_a)(1 + \varepsilon_b)(1 + \varepsilon_c)(1 + \varepsilon_e) \qquad (35)$$

where

$$1 + \varepsilon_e = \frac{R_4}{R_1} = \frac{\mathcal{M}_1}{\mathcal{M}_4} \qquad (36)$$

Values of $\varepsilon_e$ for three combustion processes at normal atmospheric pressure are shown in figure 4. The values in this figure were calculated from reference 25 assuming that $\theta_4 < 1500^\circ$ K. Below $2000^\circ$ K, dissociation effects are negligible at atmospheric pressure. The quantity $1 + \varepsilon_e$ may be calculated for other pressures and gas constituents by using the dissociation constants found in references 25 to 27 or may be obtained graphically in the range of pressures of 1/4 to 100 atmospheres by using reference 26. The composition of air at various pressures and temperatures up to $24{,}000^\circ$ K can be found in reference 28.

The effects of dissociation upon the specific heats and the entropy include not only the energies of each constituent but also include the energy of dissociation. The effect of such inclusions upon the thermodynamic properties of a diatomic gas are given in reference 29. Such effects must be included in the determination of $\varepsilon_a$ and $\varepsilon_b$.

The next question that arises at present cannot be answered with any degree of certainty. This concerns the dissociation relaxation times of the molecules. If dissociation is thought of as a large anharmonic vibration, it would be expected that the dissociation relaxation times would be comparable to the vibrational relaxation times at temperatures where there is appreciable (e.g., 10 percent) dissociation. The deviation of the vibrational relaxation time of oxygen from the theoretical curve at high temperatures may be given as evidence of this (fig. 5). However, this is contradicted by theoretical values obtained by using references 30 and 31.

For this reason the region above $2500^\circ$ K is usually avoided in this report. All experimental data concerning dissociation relaxation should be investigated before making any calculations in a temperature region of appreciable dissociation.

Other methods of measuring $P_2^*$. - The previous equations are derived with the assumption that $P_2^*$ is measured by stopping the flow in

the pneumatic probe. If the measurement is made by another probe in the moving gas stream, the equations for $1 + \varepsilon_b$ can still be used with the values of $\Sigma_b$ and $\Gamma_b$ for the probe used in the equations. However, if $P_2^*$ is measured in the plenum chamber before a supersonic nozzle ($P_2^* \equiv P_0$), and, since in the derivation $P_{Z,1}$ was taken behind a supersonic shock, an additional correction to $P_{Z,1}$ must be made to account for the entropy rise through the shock:



$$\left(\frac{P_{Z,1}}{P_2^*}\right)^2 \equiv \left(\frac{P_{Z,1}}{P_0}\right)^2 = 1 + \varepsilon_b \tag{37}$$

where from equation (8) and reference 32:

$$\ln \frac{P_2^*}{p_1} \approx c\left[1 + \psi\left(\frac{T_0}{\theta_1} - 1\right)\right] \ln \frac{T_0}{\theta_1} \tag{38}$$

and

$$\left.\begin{aligned} \frac{P_{Z,1}}{p_1} &= \left(\frac{\gamma_{P,1} + 1}{2} M_{Z,1}^2\right)^{\frac{c_{P,1}}{R}} \left(\frac{2\gamma_{P,1} M_{Z,1}^2 - \gamma_{P,1} + 1}{\gamma_{P,1} + 1}\right)^{\frac{1}{1-\gamma_{P,1}}}, \quad M_{Z,1} > 1 \\ \frac{P_{Z,1}}{p_1} &= \left(1 + \frac{\gamma_{P,1} - 1}{2} M_{Z,1}^2\right)^{c_{P,1}/R}, \quad M_{Z,1} < 1 \end{aligned}\right\} \tag{39}$$

## APPLICATION

### Determination of Relaxation Times

In order to use the previous formulas in determining the total temperature, it is necessary to find the relaxation times of the various components. The relaxation time depends upon the temperature, pressure, and the species of molecules colliding. The relaxation time of various molecules when colliding with another molecular species with a partial pressure of 1 atmosphere is shown in figure 5 as a function of the temperature. The data shown were taken from references 3, 4, 6, 7, 11, and 18. Some of these data were originally published in the form shown, other data were converted from the number of collisions required to

obtain equilibrium. The conversion was made by using the relation $\tau$ = (number of collisions)/(collision rate) and by computing the collision rate for collisions between hard spheres (ref. 33). Data on oxygen-nitrogen relaxation (not shown) may be found in references 4 and 11.

In extrapolating the data for collisions between molecules of the same species, use was made of the relation first presented by Landau and Teller (ref. 34) and expanded by Bethe and Teller (ref. 1):

$$\tau_{i,j} \propto \frac{1}{p_j} e^{\alpha\theta_p - 1/3} \tag{40}$$

(shown by solid lines in fig. 5) where $\tau_{i,j}$ is the relaxation time of molecule $i$ due to collisions with molecule $j$ and $p_j$ is the partial pressure of molecule $j$.

It has been found experimentally that for collisions between two different species the number of necessary collisions is usually almost independent of temperature. For these cases extrapolation can be made using the perfect gas law (ref. 33):

$$\tau_{i,j} \propto \frac{1}{p_j} \theta_p^{1/2} \tag{41}$$

(shown by dashed lines in fig. 5).

In a gas mixture it may also happen that the vibrational modes of a molecular species are relaxed by more than one type of collision. For example, as seen in figure 5, the relaxation of nitrogen by both nitrogen and water must be considered. In such cases the relaxation time is given by

$$\frac{1}{\tau_i} \approx \sum_j \frac{1}{\tau_{i,j}} \tag{42}$$

as the collision processes are parallel.

Figure 5 shows some disagreement between the theory (eq. (41)) and the experimental results for the relaxation of carbon dioxide by water. Much of this can probably be attributed to experimental error as relaxation times were obtained from differences in relaxation. The deviation of the data for oxygen relaxed by oxygen from theory (eq. (40)) may be attributed to anharmonic vibration or dissociation.

In all the above derivations and formulas it has been assumed that the relaxation time is constant. In fact, however, the relaxation time

is dependent on the temperature $\theta_p$ and the static pressure p. Use of such a variable relaxation time, however, would make the computations more tedious than they already are. Below Mach 1 and at temperatures above 1500° K the free-stream temperature and pressure will give a fairly accurate relaxation time. This is true because the pressure and temperature will not vary appreciably below a free-stream Mach number of 1, and in the temperature range of interest, the value of $\tau$ does not vary greatly.

At supersonic speeds this simplification will not be valid. Here, all the relaxation effects take place after the shock wave; when the velocity is once again below Mach 1, pressure and temperature will again vary inappreciably. Thus, for speeds above Mach 1, the temperature and static pressure which should be used to determine the relaxation time are those of the stream after the bow wave. Denoted by the subscript $\tau$, the pressure and temperature to be used in determining $\tau$ (from ref. 32) are given by

$$\theta_\tau \approx \theta_1, \quad M_1 < 1$$

$$\theta_\tau \approx \theta_1 \frac{\left[2\gamma_1 M_1^2 - (\gamma_1 - 1)\right]\left[(\gamma_1 - 1)M_1^2 + 2\right]}{(\gamma_1 + 1)^2 M_1^2}, \quad M_1 > 1 \tag{43}$$

$$p_\tau \approx p_1, \quad M_1 < 1 \tag{44}$$

$$p_\tau \approx p_1 \frac{2\gamma_1 M_1^2 - (\gamma_1 - 1)}{(\gamma_1 + 1)}, \quad M_1 > 1$$

## Choice of Specific Heats

After having determined the relaxation times of the various vibrational modes, it is possible to determine if such modes are to be considered unrelaxed, partially relaxed, or totally relaxed in the previous equations for $T_0$.

Whether the vibrational states of a molecule are relaxed or unrelaxed depends upon whether the relaxation time $\tau$ is short or long compared with the time taken for the molecule to change energy ($t_f$, fig. 3). This fact can also be written by using a relaxation parameter $D/u_1\tau^+$ which is approximately the ratio of these two times $t_f/\tau$. Below $D/u_1\tau^+ = 0.01$ the vibrational energy of the molecule is "frozen"

at the initial value, and $\varepsilon_a$ and $\varepsilon_b$ are equal to $\varepsilon_{a,U}$ and $\varepsilon_{b,U}$, respectively. Above $D/u_1\tau^+ = 100$ the vibrational energy of the molecule is in equilibrium with the other modes, and $\varepsilon_a$ and $\varepsilon_b$ have the values $\varepsilon_{a,R}$ and $\varepsilon_{b,R}$. Thus, when considering a gas mixture, the vibrational specific heat of those constituents which have relaxation times such that $D/u_1\tau^+ \leq 0.01$ will be given the designation $c_X$, and these vibrational specific heats will not be used in the computation of $c_B$, $c_P$, $T_Z$, $1 + \varepsilon_a$, or $1 + \varepsilon_b$. However, they will be included in $c$ when computing $T_0$ and $1 + \varepsilon_c$.

When a relaxation time is such that $D/u_1\tau^+ > 100$, these vibrational modes will be considered fully relaxed, and the vibrational specific heats of their modes are included in the specific heats $c_P$ and $c$ in all calculations.

Vibrational specific heats with relaxation times such that $0.01 < D/u_1\tau^+ < 100$ are designated $c_B$ and used in all calculations which include $c_B$, $c$, $\Psi_B$, and $T_0$.

More than one gas constituent may have vibrational modes within the region $0.01 < D/u_1\tau^+ < 100$. If the relaxation times differ by less than a factor of about three or four, the specific heats may be grouped together with a common weighted relaxation time. This can be done because both $1 + \varepsilon_a$ and $1 + \varepsilon_b$ are slowly varying functions of $D/u_1\tau^+$.

## Probe Shapes and Velocity Profiles

Once the extreme values of $\varepsilon_a$ and $\varepsilon_b$ are calculated, it becomes necessary to insert in the equations functions of the velocity profiles (eqs. (16), (17), and (25)).

A number of different probe front shapes can be used, depending upon the application of the pneumatic-probe pyrometer. Some of the possible shapes are shown in figure 6 with measured velocity profiles for these shapes at $M_1 \approx 0.7$ ($u_2/u_1 \approx 1.37$). The probe front shapes vary from flat (probes A and E) to pointed (probe C) while the constriction shape varies from a long nozzle (probe E) to an orifice (probes C and D). The resultant values of the relaxation function $(u_1/u_2)^2\Sigma_a$ obtained from these profiles are shown in figure 7 as a function of the relaxation parameter $D/u_1\tau^+$. In the region $D/u_1\tau^+ < 2$ the relaxation curve depends primarily upon the exterior probe shape, while for $D/u_1\tau^+ > 4$ the curve depends upon the shape of the constriction.

The probe shape used herein is represented by probe A in figure 6. The subsonic velocity profiles (shown in fig. 2) were measured. Above sonic free-stream velocity the velocity profiles were obtained by using reference 35 and the measured subsonic profiles. The resultant values of $(u_1/u_2)^2\Sigma_a$ and $(u_1/u_2)^2\Gamma_a$ are shown in figures 8 and 9 as functions of the parameters $u_2/u_1$ and $D/u_1\tau^+$. The values of $\Sigma_b$ and $\Gamma_b$ are shown in figures 10 and 11 as functions of $D/u_1\tau^+$ and $M_1$.

## Use of Correction Factors to Calculate Errors

Rather than make all the previously outlined corrections, the user of a pneumatic-probe pyrometer may prefer to make certain assumptions as to the state of thermal equilibrium. Thus, it would be of interest to find the error in the calculated temperature if various assumptions are used, as follows:

Method I. - Calculate relaxation times, and after finding the various values of $D/u_1\tau^+$ assume all modes with $D/u_1\tau^+ < 100$ are unrelaxed. Then use the formula:

$$T_I = (1 + \varepsilon_c)\left(\frac{A_2P_2^*}{A_4P_4^*}\right)^2 T_4^*\left[\frac{h(\gamma_{P,1})}{h(\gamma_4)}\right] \tag{45}$$

The error in the calculated $T_I$ is

$$\frac{T_0 - T_I}{T_0} \approx \varepsilon_a + \varepsilon_b + \varepsilon_c \tag{46}$$

Method II. - Calculate relaxation times, and after finding the various values of $D/u_1\tau^+$ assume all modes with $D/u_1\tau^+ > 0.01$ are fully relaxed. Then use the formula:

$$T_{II} = \left(\frac{A_2P_2^*}{A_4P_4^*}\right)^2 T_4^*\left[\frac{h(\gamma_1)}{h(\gamma_4)}\right] \tag{47}$$

Then, the error in $T_{II}$ is given by:

$$\frac{T_0 - T_{II}}{T_0} \approx \varepsilon_a + \varepsilon_b + \varepsilon_c + \varepsilon_d + \varepsilon_e \tag{48}$$

where

$$1 + \varepsilon_d = \frac{h(\gamma_{P,1})}{h(\gamma_1)} \tag{49}$$

Method III. - Assume all the modes are unrelaxed to the extent that $T_{Z,1} \approx T_0$ and that $\gamma_{P,1} \approx \gamma_4$, then use the formula:

$$T_{III} = \left(\frac{A_2 P_2^*}{A_4 P_4^*}\right)^2 T_4^* \tag{50}$$

The error is given by:

$$\frac{T_0 - T_{III}}{T_0} \approx \varepsilon_a + \varepsilon_b + \varepsilon_c + \varepsilon_d + \varepsilon_e \tag{51}$$

where

$$1 + \varepsilon_d = \frac{h(\gamma_{P,1})}{h(\gamma_4)} \tag{52}$$

Method IV. - Another method that can be used is to assume some sort of "effective $\gamma$" for the process. Then

$$T_{IV} = \left(\frac{A_2 P_2^*}{A_4 P_4^*}\right) T_4^* \frac{h(\gamma_{eff})}{h(\gamma_4)} \tag{53}$$

where

$$\frac{h(\gamma_{P,1})}{h(\gamma_{eff})} \approx 1 + \varepsilon_a + \varepsilon_b + \varepsilon_c + \varepsilon_e = \frac{T_0}{T_{IV}} \tag{54}$$

Comparison of methods. - The general shapes of the error curves as a function of a relaxation parameter $D/\tau^+\sqrt{\gamma_{P,1}R\theta_1}$ are shown in figures 12 and 13. In order to calculate these curves the following assumptions were made: $c_{P,1}/R = 4.0$, $c_1/R = 4.5$, and $c_1/R = 3.5$. The parameter, diameter divided by relaxation time multiplied by free-stream sonic velocity, $D/\tau^+\sqrt{\gamma_{P,1}R\theta_1}$ is used to place the curves on a common ordinate. A displacement of these curves upward or downward may be expected from changes in heat capacities.

By using the curves in figure 12 as a guide, the following tabulation can be made of the "best" method to be used in each region of relaxation. For $M_1 < 0.5$:

$D/\tau^+\sqrt{\gamma_{P,1}R\theta_1} < 10$, method I

$D/\tau^+\sqrt{\gamma_{P,1}R\theta_1} > 10$, method II

$D/\tau^+\sqrt{\gamma_{P,1}R\theta_1} < 10$ and $(c_{P,1} - c_4)/c_{P,1} < 0.05$, method III

$D/\tau^+\sqrt{\gamma_{P,1}R\theta_1} > 10$ and $(c_1 - c_4)/c_1 < 0.05$, method III

Above $M_1 = 0.5$, either $D/\tau^+\sqrt{\gamma_{P,1}R\theta_1}$ or $D/u_1\tau^+$ may be used to determine the best method by using the previous tabulation.

The variation of effective $\gamma$ in figure 13 with Mach number should be noted. The way in which this term varies with Mach number depends to a large extent upon the degree of relaxation.

CS-3 back

## Other Applications of Formulas

Since $1 + \varepsilon_a$ is the mass-flow rate correction, it can be used to determine $m_2$.

To find $m_2$ as a function of $P_{Z,1}$ and $T_{Z,1}$, use equation (B25) in appendix B and equation (17).

To find $m_2$ as a function of $P_0$ and $T_0$, use equations (B25), (33), and (37).

Since $1 + \varepsilon_b$ is the pressure measurement correction, it can be used to determine $P_2^*$.

To find $P_2^*$ in terms of $P_{Z,1}$ and $T_{Z,1}$, use equations (B42) and (25).

To find $P_2^*$ in terms of $P_0$ and $T_0$, use equations (B40), (25), (33), and (37).

### Limitations of Equations

The formulas in the text and in appendix B can be used for a number of flow processes besides those of the pneumatic-probe pyrometer. There are, however, certain limitations to the unmodified application of these formulas.

(1) Above 4000° K the dissociation relaxation times of nitrogen and oxygen become short enough to be comparable to the vibrational relaxation times.

(2) When the mean free path of the molecules becomes comparable to the nozzle diameter, the continuous flow equations are no longer applicable.

(3) Above $M_1 \approx 2.0$ the rise in entropy across the shock is of such magnitude that the use of the expansion $e^{-\Delta S} \approx 1 - \Delta S$ becomes doubtful.

(4) When the equations are used to calculate long nozzle flow (supersonic diffusers) and $M_1 > 2$, the relaxation times cannot be considered constant, and the evaluation must be made stepwise.

(5) Above $M_1 \approx 2$ the specific heats of the process cannot be considered as simply as in equation (8).

For the above reasons the upper limit of usefulness of these equations when used with pneumatic probes is given by $p_1 \geq 3 \times 10^{-3}$ atmosphere, $M_1 \leq 2$, and $\theta_1 \leq 3000°$ K. These formulas can probably be used with due caution for estimation purposes to $p_1 = 3 \times 10^{-4}$ atmosphere, $M_1 = 4$, and $\theta_1 = 4000°$ K.

## EXAMPLES

By using the previous equations and the equations in the appendixes, three examples will be shown. In calculating values of $\Sigma_a$ and $\Sigma_b$ the measured profiles will be used; thus, the results shown are for a probe with a shape similar to that shown in figure 2 (or probe A of fig. 6) with a 4-to-1 probe-to-throat diameter ratio.

### Example 1, Products of Combustion of a Heavy Hydrocarbon and Air

The computation of one point in this example is shown in appendix C. Figure 14 shows the error by using the four methods. As the free-stream pressure was assumed atmospheric and the temperature was assumed

to be 1500° K, all dissociation effects could be neglected. The curves are plotted as a function of the free-stream Mach number $M_1$. The values of specific heats and $\psi$ used are those given in tables I and II.

This example is of special interest because of the experimental data available at present on the use of pneumatic probes in measuring temperatures in hydrocarbon-air flames (refs. 21 to 23). The curves in figure 14 substantiate the general conclusions for this shape of probe drawn from the previous figures.

In reference 21 method III was used and was considered accurate. However, the probe shapes of reference 21 and this report were different. The ratio of probe diameters in reference 21 was as high as 8 to 1, and the constriction used was an orifice. Thus, compared with the present probe more stagnation occurred in front of the reference probe, which made the unrelaxed portion of the curves for $\Sigma_a$ longer (see fig. 7). The result was that the nitrogen modes were unrelaxed, and the carbon dioxide and water modes were partially relaxed. For this reason the curve for the first three methods (applied to the probe of ref. 21) would be raised higher, probably by about 0.01 to 0.015, and the dependency of these curves upon the free-stream Mach number would be less. The curve for the effective $\gamma$ would become more horizontal and would have a value larger than $\gamma_{P,1}$. From figure 7 in reference 21 it can be assumed that the measured temperatures were accurate to within 2 percent. The raising of the error curves would place the curve for method III within this limit.

In reference 23 an effective $\gamma$ which is varied from $\gamma_4$ at $M_1 = 0$ to $\gamma_1$ at $M = 1.0$ is used. The comparison between the calculations as shown in figure 14 and the results of reference 23 should be direct as the sizes and shapes of the probes are similar. While the trend in the effective $\gamma$ given in figure 14 is the same as that given in reference 23, the magnitude of the change is different. Such a magnitude of a change in effective $\gamma$ in figure 14 could only be accomplished if the relaxation times were 100 times longer for water and carbon dioxide than that given in figure 5. Thus, this discrepancy can only be attributed to other effects not considered in this paper, probably heat-transfer effects at low Mach numbers.

In spite of these differences, figure 14 shows that, because of the high percentage of nitrogen in the combustion system, the use of any of the four methods does not entail any large errors over a range of subsonic and low supersonic Mach numbers.

Example 2, Supersonic Flow of Combustion Products of Ammonia and Oxygen

Figure 15 shows the errors when the various methods are used. Again, the errors are plotted as a function of the free-stream Mach number $M_1$.

For this case atmospheric pressure is again assumed along with a free-stream static temperature of 2000° K. Effect of dissociation is once more ignored (see fig. 6). The probe diameter assumed was $D \approx 3/4$ inch. In this example the vibrational modes of water could be considered relaxed as $D/u_1\tau^+ > 1500$. The values of $D/u_1\tau^+$ for the nitrogen ranged from 9 to 25. Because of the large changes in temperature and, thus, specific heats at these Mach numbers, the values of $\psi_P$ and $\psi_B$ were calculated from reference 32 by using a larger temperature range than that used to obtain table II.

This example is of interest because it shows what may happen as more complex propellants and higher Mach numbers are used. As the higher Mach numbers are reached, both methods II and I are in error.

The downward displacement of the error in method II must also be noted. This displacement is due to the use of the free-stream relaxed $\gamma$ in method II where the $\gamma$ of the process is more nearly the $\gamma$ given by the specific heats behind the shock.

### Example 3, Effects of Relaxation on Critical Velocity

Figure 16 shows the effects of relaxation on the critical velocity in the first nozzle. Because of the assumption of constant critical velocity, the approximate methods cannot be used. However, the critical velocities were calculated for some conditions by using the iteration method. Figure 16 shows that the transition from the unrelaxed critical velocity $u_{U,2}$ to the critical velocity with complete thermal equilibrium is not a smooth one, especially in the region $M_1 \approx 1$ and $D/u_1\tau^+ < 10$.

## CONCLUDING REMARKS

Equations are derived which evaluate the effects of thermal vibrational relaxation and specific-heat changes on pneumatic-probe pyrometer measurements in the region to 3000° K and Mach number $< 2.0$. By using these derived equations, a simpler working set of equations is given which are shown to be adequately accurate.

Methods are given by which the results of these equations may be used to determine the error in temperature measurement if different assumptions are made as to the state of thermal equilibrium of the gas in the probe. By using these methods, examples are given for a typical probe. Different assumptions must be made, depending upon the velocity, probe size, and gas constituents. The results are in partial agreement with the experimental evidence obtained in other reports.

The relaxation error entailed by using any of the methods will not be large for the case of hydrocarbon combustion in air in the region of free-stream static temperature $< 2500^{\circ}$ K and free-stream Mach number $< 1.2$.

The calculation of one point in one example is given as a sample calculation. The limitations of the equations presented and corrections for dissociation are discussed. The effect of partial relaxation upon the critical velocity is also shown.

4205

Lewis Flight Propulsion Laboratory
National Advisory Committee for Aeronautics
Cleveland, Ohio, May 13, 1957

## APPENDIX A

## SYMBOLS

| | |
|---|---|
| A | effective nozzle area |
| B | coefficient |
| c | specific heat at constant pressure, $(\partial E/\partial \theta)_p$ |
| D | probe outside diameter |
| d | nozzle-throat diameter |
| E | thermal energy (enthalpy) |
| F | coefficient |
| $h(\gamma)$ | $h(\gamma) = \gamma\left(\frac{2}{\gamma+1}\right)^{\frac{\gamma+1}{\gamma-1}}$ (eq. (13)) |
| M | Mach number |
| $\mathcal{M}$ | molecular weight |
| m | mass-flow rate (eq. (6)) |
| n | polytropic gas exponent (eq. (10)) |
| P | total pressure |
| p | static pressure |
| R | specific gas constant |
| S | entropy |
| T | total temperature |
| $T_0$ | true total temperature (eq. (3)) |
| t | time |
| $t_f$ | time at point of critical flow (eq. (15)) |
| u | velocity |

$\alpha$ exponential coefficient (eq. (40))

$\beta$ correction exponent (eqs. (18), (22), (27), and (31))

$\Gamma$ relaxation integral (eq. (16))

$\gamma$ ratio of specific heats, $c/(c - R)$

$\varepsilon$ correction factor (eq. (12))

$\theta$ static temperature

$\rho$ density

$\Sigma$ relaxation integral (eq. (15))

$\tau$ relaxation time (eqs. (1) and (2))

$\tau^+$ modified relaxation time, $\tau \frac{c_{P,1}}{c_{P,1} + c_{B,1}}$

$\psi$ specific-heat function, $\frac{1}{2}\left(\frac{d\dot{c}}{d\theta}\right)_1\left(\frac{\theta_1}{c_1}\right)$ (eq. (9))

Subscripts:

eff effective

i,j mode of molecular species (used with c, $\tau$, and $\psi$ to denote a particular mode or species in a general equation)

0,1,2, 3,4 position in probe as shown in fig. 1 (used with A, c, E, M, P, p, T, U, $\gamma$, $\theta$, and $\rho$ to denote at which physical position the quantity is taken)

I,II, III,IV calculation method (used with T to denote method by which total temperature is calculated)

The following subscripts are used with $\varepsilon$, $\Sigma$, and $\Gamma$ to denote type of correction:

a critical flow correction

b total-pressure measurement correction

c correction to true total temperature

d $\gamma$ correction

e dissociation correction

The following subscripts are used with c, E, M, P, p, T, $\theta$, and $\psi$ to denote assumed relaxation state of the variables:

B vibrational mode when partially relaxed

P relaxed modes when partially relaxed vibrational mode is partially relaxed

R relaxed modes when partially relaxed vibrational mode is relaxed

U relaxed modes when partially relaxed vibrational mode is unrelaxed

X relaxed modes

Z relaxed modes when partially relaxed vibrational mode is unrelaxed and specific heats are independent of temperature

Superscripts:

B,P, R,U temperature state (used with E and $\theta$ to denote temperature state at which a mode is to be taken when that temperature state is not that normally assumed by the mode)

* measured quantity (used with P, T, $\beta$, $\theta$, and $\rho$ to denote a measured quantity and/or a quantity when flow through nozzle is stopped)

## APPENDIX B

### PNEUMATIC-PROBE PYROMETER EQUATIONS WITH RELAXATION

In finding the relations between the measured quantities $P_2^*$, $T_4^*$, and $P_4^*$ and the total temperature $T_0$, five equations must be satisfied:

(1) Energy conservation (eq. (B1))

(2) Critical flow (eq. (B6))

(3) Entropy (eq. (B8))

(4) Relaxation (eq. (2))

(5) Conservation of mass (eq. (B43))

In order to obtain a workable solution to these five equations, four assumptions are made:

(1) Specific heat is a linear function of temperature:

$$c_i = c_{i,1} + 2c_{i,1}\psi_i \left(\theta_i/\theta_1 - 1\right)$$

where $\psi << 1$.

(2) Static pressures and temperatures are related by

$$\frac{p_2}{p_1} = \left(\frac{\theta_{P,2}}{\theta_1}\right)^{n/n-1}$$

(3) Relaxation time $\tau$ is constant over the process.

(4) All modes are in equilibrium at station 1:

$$\theta_1 = \theta_{P,1} = \theta_{B,1} = \theta_{X,1}$$

#### Energy, Velocity, and Mass Flow

The equation for the energy at station 2 (eq. (5)) is written as

$$E_{P,2} + E_{B,2} + E_{X,1} + \frac{u_2^2}{2} = E_{P,1} + E_{B,1} + E_{X,1} + \frac{u_1^2}{2} = c_{P,1}T_{Z,1} + E_{B,1} + E_{X,1} \tag{B1}$$

or, by solving for $u_2$:

$$u_2^2 = 2c_{P,1}\theta_1\left(\frac{T_{Z,1}}{\theta_1} + \frac{E_{B,1} - E_{B,2}}{c_{P,1}\theta_1} - \frac{E_{P,2}}{c_{P,1}\theta_1}\right) \tag{B2}$$

From assumption (2)

$$\frac{P_{Z,1}}{p_2} = \left(\frac{T_{Z,1}}{\theta_1}\right)^{\frac{c_{P,1}}{R}}\left(\frac{\theta_1}{\theta_{P,2}}\right)^{\frac{n}{n-1}} \tag{B3}$$

where for supersonic gas flow $P_{Z,1}$ is taken after the bow shock.

By using equation (B3) the mass-flow rate is given by

$$m_2 = A_2\rho_2 u_2 = \frac{AP_{Z,1}}{\sqrt{RT_{Z,1}}}\left(\frac{\theta_1}{T_{Z,1}}\right)^{\frac{1}{\gamma_{P,1}-1}}\left(\frac{\theta_{P,2}}{\theta_1}\right)^{\frac{1}{n-1}}\frac{u_2}{\sqrt{RT_{Z,1}}} \tag{B4}$$

Substituting equation (B2) into (B4) and collecting terms give

$$m_2 = \frac{A_2P_{Z,1}}{\sqrt{RT_{Z,1}}}\sqrt{\frac{2c_{P,1}}{R}\left(\frac{\theta_1}{T_{Z,1}}\right)^{\frac{2c_{P,1}}{R}}}\sqrt{\left(\frac{T_{Z,1}}{\theta_1} + \frac{E_{B,1} - E_{B,2}}{c_{P,1}\theta_1}\right)\left(\frac{\theta_{P,2}}{\theta_1}\right)^{\frac{2}{n-1}} - \left(\frac{\theta_{P,2}}{\theta_1}\right)^{\frac{n+1}{n-1}}\frac{E_{P,2}}{c_{P,1}\theta_{P,2}}} \tag{B5}$$

## Critical Flow and Entropy

For critical flow $dm_2/dp_2 = 0$ (eq. (6)) or because of assumption (2),

$$\partial m_2/\partial\theta_{P,2} = 0 \tag{B6}$$

Thus, by differentiating equation (B5), the following equation is obtained:

$$\frac{2}{n-1}\left(\frac{T_{Z,1}}{\theta_1} + \frac{E_{B,1}-E_{B,2}}{c_{P,1}\theta_1}\right) - \frac{n+1}{n-1}\frac{E_{P,2}}{c_{P,1}\theta_1} - \left(\frac{\theta_{P,2}}{\theta_1}\right)^2\theta_1\frac{\partial\left(E_{P,2}/c_{P,1}\theta_{P,2}\right)}{\partial\theta_{P,2}} -$$

$$\frac{2\theta_{P,2}}{(n-1)^2}\left(\ln\frac{\theta_{P,2}}{\theta_1}\right)\left(\frac{T_{Z,1}}{\theta_1} + \frac{E_{B,1}-E_{B,2}}{c_{P,1}\theta_1} - \frac{E_{P,2}}{c_{P,1}\theta_1}\right)\frac{dn}{\partial\theta_{P,2}} - \frac{\theta_{P,2}}{\theta_1}\frac{1}{c_{P,1}}\frac{\partial E_{B,2}}{\partial\theta_{P,2}} = 0 \tag{B7}$$

Equation (B7) has three variables, $E_{P,2}$, $E_{B,2}$, and n. In order to eliminate n an equation for the entropy change is used. From equation (7a) of reference 10 or from the entropy relations of reference 6:

$$\ln \frac{p_2}{p_1} = - \int_1^2 \frac{1}{2} \frac{du^2}{\theta_P} = \int_1^2 \frac{dE_B}{\theta_B} + \frac{dE_P}{\theta_P} - \Delta S \tag{B8}$$

Using equation (B1) and assumption (2) gives

$$\ln \frac{p_2}{p_1} = \frac{n}{n-1} \ln \frac{\theta_{P,2}}{\theta_1} = - \int_1^2 dE_B \left( \frac{1}{\theta_B} - \frac{1}{\theta_P} \right) + \int_1^2 \frac{dE_B}{\theta_B} + \frac{dE_P}{\theta_P} \tag{B9}$$

By using assumption (1), equation (B9) may be written:

$$\ln \left( \frac{n}{n-1} \right) R \ln \frac{\theta_{P,2}}{\theta_1} = c_{P,1} \ln \frac{\theta_{P,2}}{\theta_1} \left[ 1 + 2\psi_P \left( \frac{\frac{\theta_{P,2}}{\theta_1} - 1}{\ln \frac{\theta_{P,2}}{\theta_1}} - 1 \right) \right] +$$

$$c_{B,1} \ln \frac{\theta_{B,2}}{\theta_1} \left[ 1 + 2\psi_B \left( \frac{\frac{\theta_{B,2}}{\theta_1} - 1}{\ln \frac{\theta_{B,2}}{\theta_1}} - 1 \right) \right] - \int_1^2 dE_B \left( \frac{1}{\theta_B} - \frac{1}{\theta_P} \right) \tag{B10}$$

## Relaxation Equations

If equations (B5) and (B7) are used to calculate the mass-flow rate $m_2$, the variables $\theta_{B,2}$ and $\theta_{P,2}$ must also be determined as functions of the state of thermal equilibrium.

The third equation which must be satisfied is the relaxation equation

$$\frac{d}{dt} E_B = - \frac{1}{\tau} (E_B - E_B^P) \tag{2}$$

If it is assumed that $c_B/c_P \approx c_{B,1}/c_{P,1}$ over the process, equation (2) may be written:

$$\frac{\partial}{\partial t}\left(E_B - E_B^P\right) \approx \frac{1}{\tau^+}\left(E_B - E_B^P\right) \tag{B11}$$

where

$$\tau^+ = \tau \frac{c_{P,1}}{c_{P,1} + c_{B,1}} \tag{B12}$$

By defining

$$E_R \equiv E_U + E_{B,1} + E_{X,1} = E_P + E_B + E_X \tag{B13}$$

$$E_R^U \equiv E_U + E_B^U + E_{X,1} \tag{B14}$$

$$E_R^P \equiv E_P + E_B^P + E_{X,1} \tag{B15}$$

the solution to equation (B11) may be written as

$$E_{R,2}^P = E_{R,2} + \int_0^{t_f}\left[\frac{\partial}{\partial t}\left(E_R^U - E_R\right)\right] e^{(t_f - t)/\tau^+}\, dt \tag{B16}$$

Using assumption (1) and rewriting the equation in terms of the free-stream Mach number $M_1$ and the velocity ratio $u_2/u_1$ give

$$\left(\frac{\theta_{P,2}}{\theta_1} - 1\right)\left[1 + \left(\frac{c_{P,1}\psi_P + c_{B,1}\psi_B}{c_{P,1} + c_{B,1}}\right)\left(\frac{\theta_{P,2}}{\theta_1} - 1\right)\right] \approx \frac{\gamma_1 - 1}{2} M_1^2\left[1 - \left(\frac{u_2}{u_1}\right)^2\right] - \frac{c_{B,1}}{c_1}\left(\frac{\gamma_1 - 1}{2} M_1^2\right) B\Sigma_a + \frac{c_{B,1}}{c_1}\left(\frac{\gamma_1 - 1}{2} M_1^2\right) F\Sigma_{aa} \tag{B17}$$

where

$$B \approx 1 + 2\left(\frac{\gamma_1 - 1}{2} M_1^2\right)\left(\psi_B - \psi_P\right) - 6\psi_P\left(\frac{\gamma_1 - 1}{2} M_1^2\right)\left(\psi_B - \psi_P\right) \tag{B18}$$

$$F \approx \left(\psi_B - \psi_P\right) - 6\psi_P\left(\frac{\gamma_1 - 1}{2} M_1^2\right)\left(\psi_B - \psi_P\right) \tag{B19}$$

$$\Sigma_a = \int_0^{t_f}\left[\frac{d}{dt}\left(\frac{u}{u_1}\right)^2\right] e^{(t - t_f)/\tau^+}\, dt \tag{B20}$$

$$\Sigma_{aa} = \int_0^{t_f} \left[\frac{d}{dt}\left(\frac{u}{u_1}\right)^4\right] e^{(t-t_f)/\tau^+} dt \tag{B21}$$

By using equations (B2), (B7), (B10), and (B17) a unique solution for the variables $\theta_{P,2}$, $\theta_{B,2}$, and $u_2$ for critical flow can be obtained. However, such a solution is a tedious process requiring double iteration and usually necessitating the use of an electronic computer.



## Introduction of $1 + \varepsilon_a$

The first step toward any simplification or approximation is to write the equation for mass-flow rate in such a way that the effects of approximations can be easily seen.

Rather than attempt to express equation (B7) in terms of (B10), another form of equation (B5) can be used. The following variables are introduced:

$$u_{Z,2}^2 = 2\frac{\gamma_{P,1}}{\gamma_{P,1}+1} RT_{Z,1} \tag{B22}$$

$$\frac{\theta_{Z,2}}{\theta_1} = \frac{T_{Z,1}}{\theta_1}\frac{2}{\gamma_{P,1}+1} \tag{B23}$$

These would be the solutions of equations (B2) and (B7) if there were no partially relaxed modes ($E_B = 0$) and no specific-heat changes with temperature ($E_{P,2} = c_{P,1}\theta_{Z,2}$).

Inserting equations (B10) and (2) into (B4) gives

$$m_2 = \frac{AP_{Z,1}}{\sqrt{RT_{Z,1}}} \sqrt{h(\gamma_{P,1})(1+\varepsilon_a)} \tag{B24}$$

where

$$h(\gamma_{P,1}) = \left(\frac{\theta_{Z,2}}{T_{Z,1}}\right)^{\frac{2}{\gamma_{P,1}-1}} \left(\frac{u_{Z,2}}{\sqrt{RT_{Z,1}}}\right)^2 = \gamma_{P,1}\left(\frac{2}{\gamma_{P,1}+1}\right)^{\frac{\gamma_{P,1}+1}{\gamma_{P,1}-1}} \tag{B25}$$

$$1 + \varepsilon_a = \left(\frac{\theta_{P,2}}{\theta_{Z,1}}\right)^{\frac{2}{\gamma_{P,1}-1}} \left(\frac{\theta_{P,2}}{\theta_1}\right)^{2\beta} \left(\frac{u_2}{u_{Z,2}}\right)^2 e^{-2\Delta S_a/R} \tag{B26}$$

where

$$\Delta S_a = \int_1^2 dE_B \left(\frac{1}{\theta_B} - \frac{1}{\theta_P}\right) \tag{B27}$$

and where, from equation (B9),

$$\beta \approx \frac{c_{P,1}\psi_P}{R}\left(\frac{\theta_{P,2}}{\theta_1} - 1\right) + \frac{c_{B,1}}{c_{P,1}} \frac{\ln \frac{\theta_{B,2}}{\theta_1}}{\ln \frac{\theta_{P,2}}{\theta_1}} \left[1 + \psi_B\left(\frac{\theta_B}{\theta_1} - 1\right)\right] \tag{B28}$$

The equation equivalent to (B7) is written as

$$\frac{\partial(1 + \varepsilon_a)}{\partial\theta_{P,2}} = 0 \tag{B29}$$

For the solution of equation (B27) it is still necessary to satisfy equations (B2), (B7), (B10), and (B17). To simplify the solution additional assumptions will be made.

If the integral in equation (B10), which is equal to $-\Delta S_a$, is assumed equal to zero, n and $dn/d\theta_{P,2}$ may be expressed explicitly in terms of $\theta_{P,2}$ and $\theta_{B,2}$. By using the more simple equations which result from the assumption of $\psi = 0$, it was found that such an assumption as to the entropy could be used to determine the critical velocity and thus $(1 + \varepsilon_a)e^{\Delta S_a/R}$ at Mach numbers below $M_1 = 1.4$. Such an assumption as to the entropy leads to the rewriting of equation (B7) in the form:

$$\left[2\left(\frac{T_{Z,1}}{\theta_1} + \frac{E_{B,1} - E_{B,2}}{c_{P,1}\theta_1} - \frac{E_{P,2}}{c_{P,1}\theta_1}\right)\right]\left[1 - \frac{1}{R}\left(\frac{\theta_{P,2}}{\theta_{B,2}}\frac{\partial E_{B,2}}{\partial\theta_{P,2}} + \frac{\partial E_{P,2}}{\partial\theta_{P,2}}\right)\right] -$$

$$\left[\frac{\theta_{P,2}}{c_{P,1}\theta_1}\left(\frac{\partial E_{B,2}}{\partial\theta_{P,2}} + \frac{\partial E_{P,2}}{\partial\theta_{P,2}}\right)\right] = 0 \tag{B30}$$

where from assumption (1)

$$\frac{\partial E_{P,2}}{\partial \theta_{P,2}} = c_{P,1} + 2\psi_P c_{P,1}\left(\frac{\theta_{P,2}}{\theta_1} - 1\right) \tag{B31}$$

and

$$\frac{\partial E_{B,2}}{\partial \theta_{P,2}} = \frac{c_{P,1}}{c_{P,1}\dfrac{\partial \theta_{P,2}}{\partial E_{U,2}}} - \frac{c_{P,1}\partial E_{P,2}}{\partial \theta_{P,2}} \tag{B32}$$

By using equations (B30) to (B32), (B2), (B17), and (B26), the value of $(1 + \varepsilon_a)e^{2\Delta S_a/R}$ is found for any given state of relaxation. This was done using an iteration process on an IBM 650 digital computer. Some of the results are shown in figure 17.

Also shown in the figure is the function $(1 + \varepsilon_a)e^{2\Delta S_a/R}$ when this is computed by the method given in the text:

$$(1 + \varepsilon_a)e^{2\Delta S_a/R} = 1 + \varepsilon_{a,U} + \left[1 - \frac{\Sigma_a}{(u_2/u_1)^2 - 1}\right](\varepsilon_{a,R} - \varepsilon_{a,U}) \tag{B33}$$

As is seen, this is a good approximation.

Next it is necessary to compute the factor $e^{-2\Delta S_a/R}$. This was done in the following manner:

In the special case where $\psi = 0$, $\Delta S_a$ can be rewritten with the aid of the relaxation equation (2):

$$\Delta S_a = \int_1^2 dE\left(\frac{1}{\theta_B} - \frac{1}{\theta_P}\right) = \frac{1}{2}\left(\frac{\gamma - 1}{2} M_1^2\right)^2 \frac{c}{c_P} c_B \Gamma_a \tag{B34}$$

where

$$\Gamma_a \simeq \frac{2}{\left(\dfrac{\gamma - 1}{2} M_1^2\right)} \frac{1}{\tau^+} \int_{t_1}^{t_f} \left(\frac{\theta_R - \theta_B}{\theta_R}\right)^2 dt \simeq \frac{2}{\tau^+} \int_{t_1}^{t_f} \left[\frac{\Sigma_a(t)}{\theta_R/\theta_1}\right]^2 dt \tag{B35}$$

Since $e^{-2\Delta S_a/R} \approx 1 - 2\Delta S_a/R$,

$$e^{-2\Delta S_a/R} \approx 1 - \left(\frac{\gamma - 1}{2} M_1^2\right)^2 \frac{c_1}{c_{P,1}} \frac{c_{B,1}}{R} \Gamma_a \tag{B36}$$

which is modified to the following when there is a change in specific heat with temperature:

$$e^{-2\Delta S_a/R} \approx 1 - \left(\frac{\gamma - 1}{2} M_1^2\right)^2 \frac{c}{c_P} \frac{c_B}{R} \Gamma_a \left[1 + 2\left(\frac{\gamma - 1}{2} M_1^2\right)(\psi_B - \psi_P)\right] \tag{B37}$$

In most cases equation (B36) is sufficiently accurate.

Combining equations (B33) and (B36) gives

$$\varepsilon_a = \varepsilon_{a,U} + \left(1 - \frac{\Sigma_a}{(u_2/u_1)^2 - 1}\right)(\varepsilon_{a,R} - \varepsilon_{a,U}) - \left(\frac{\gamma - 1}{2} M_1^2\right)^2 \frac{c}{c_P} \frac{c_B}{R} \Gamma_a \tag{B38}$$

and repeating equation (B24) results in

$$m_2 = \frac{AP_{Z,1}}{\sqrt{RT_{Z,1}}} \sqrt{h(\gamma_{P,1})(1 + \varepsilon_a)} \tag{B24}$$

Values of $(u_1/u_2)^2 \Sigma_a$ as a function of $D/u_1\tau^+$ and $u_2/u_1$ are shown in figures 7 and 8. Values of $(u_1/u_2)^4 \Gamma_a$ as a function of $D/u_1\tau^+$ and $u_2/u_1$ are shown in figure 9.

## Introduction of $1 + \varepsilon_b$

The flow in the probe was stopped, and $P_2^*$ was measured. This measured value of $P_2$ is used in the equation for mass-flow rate (eq. (B25)) which is now written:

$$m_2 = \frac{A_2 P_2^*}{\sqrt{RT_{Z,1}}} \sqrt{h(\gamma_{P,1})(1 + \varepsilon_a)(1 + \varepsilon_b)} \tag{B39}$$

where

$$1 + \varepsilon_b = \left(\frac{P_{Z,1}}{P_2^*}\right)^2 \tag{B40}$$

or, by using the entropy equation (B9) and the form of (B26) and (B28)

$$1 + \varepsilon_b = \left(\frac{T_{Z,1}}{T_2^*}\right)^{2c_{P,1}/R} \left(\frac{\theta_1}{T_2^*}\right)^{2\beta^*} e^{2\Delta S_b/R} \tag{B41}$$

where

$$\Delta S_b = \int_1^2 dE_B^* \left(\frac{1}{\theta_B^*} - \frac{1}{\theta_P^*}\right) \tag{B42}$$

$$\beta \approx \frac{c_{P,1}\psi_P}{R}\left(\frac{T_2^*}{\theta_1} - 1\right) + \frac{c_{B,1}}{c_{P,1}} \frac{\ln \frac{\theta_{B,2}^*}{\theta_1}}{\ln \frac{T_2^*}{\theta_1}} \left[1 + \psi_B\left(\frac{\theta_B^*}{\theta_1} - 1\right)\right] \tag{B43}$$

Since it is not necessary to determine $u_2/u_1$ for this case, $T_2^*$ may be obtained directly from a modified form of equation (B17) in which:

(1) $\theta_{P,2}$ is replaced by $T_2^*$

(2) $\Sigma_a$ is replaced by $\Sigma_b$

(3) $\Sigma_{aa}$ is replaced by $\Sigma_{bb}$

By using the equation for conservation of energy $\theta_{B,2}^*$ is determined. Thus, $T_2^*$, $\theta_{B,2}^*$, and $\beta^*$ can be calculated.

The correction equation (25) may be obtained in the following manner:

For the special case of $\psi = 0$ the pressure $P_2^*$ is obtained from the entropy equation (B9):

$$\ln \frac{P_2^*}{p_1} = \int_1^2 c_B \, d\theta_B \left(\frac{1}{\theta_B} - \frac{1}{\theta_P}\right) + \int_1^2 c_B \frac{d\theta_B}{\theta_B} + c_P \frac{d\theta_P}{\theta_P} \tag{B44}$$

$$= \int_1^2 c_B \, d\theta_B \left(\frac{1}{\theta_B} - \frac{1}{\theta_P}\right) + c_B \ln \frac{\theta_{B,2}}{\theta_1} + c_P \ln \frac{\theta_{P,2}}{\theta_1} \tag{B45}$$

Using once more the relaxation equation (25) as was done in equation (B34) and expanding the last two terms in the previous equation give

$$\ln \frac{P_2^*}{p_1} \approx \frac{c_B}{\tau^+} \left(\frac{c}{c_P}\right) \left(\frac{\gamma - 1}{2} M_1^2\right)^2 \int_{t_1}^{t_f} \left(\frac{\Sigma_b(t)}{\theta_R/\theta_1}\right)^2 dt + c \ln \frac{\theta_R}{\theta_1} + c_B \left(\frac{c}{c_P}\right) \left(\frac{\theta_1}{\theta_{R,2}}\right)^2 \left(\frac{\gamma - 1}{2} M_1^2\right)^2 \Sigma_b^2 \tag{B46}$$

$$\ln \frac{P_2^*}{p_1} \approx c \ln \frac{\theta_R}{\theta_1} + c_B \left(\frac{c}{c_P}\right) \left(\frac{\gamma - 1}{2} M_1^2\right)^2 \left(\frac{\theta_1}{\theta_{R,2}}\right)^2 (\Sigma_b^2 + \Gamma_b) \tag{B47}$$

where

$$\Gamma_b = \left(\frac{\theta_{R,2}}{\theta_1}\right)^2 \frac{1}{\tau^+} \int_{t_1}^{t_f} \left(\frac{\Sigma_b(t)}{\theta_R/\theta_1}\right)^2 dt \tag{B48}$$

The pressure $P_2^*/p_1$ is given in the form $A + B(\Sigma_b^2 + \Gamma_b)$ which, when inserted into equation (B40) and in turn normalized for the extremes, is the same as equation (25):

$$\varepsilon_b = \varepsilon_{b,U} + (1 - \Sigma_b^2 - \Gamma_b)(\varepsilon_{b,R} - \varepsilon_{b,U}) \tag{25}$$

The calculated values of $\Gamma_b$ are shown in figure 11 as a function of $D/u_1\tau^+$ and $M_1$. In the range $0.3 < M_1 < 1.4$ the values of $\Gamma_b$ for different specific heats were equal to within 10 percent of those shown.

Figure 10 shows the calculated values of $\Sigma_b$ as a function of $D/u_1\tau^+$. A comparison of the function $(1 + \varepsilon_b)e^{-2\Delta S_b}$ calculated from equation (B41) and from equation (25) is shown in figure 18. The agreement is good.

## Flow through Second Nozzle

The second nozzle is used as a method of measuring the mass-flow rate. If it is assumed that the gas temperature at this nozzle is low ($\theta_3 < 500^\circ$ K), the usual equations for critical flow through a nozzle can be used (refs. 19 to 23):

$$m_4 = \frac{A_4 P_4^*}{\sqrt{RT_4^*}} h(\gamma_4) \tag{B49}$$

## Final Equation

If mass is conserved through the probe,

$$m_2 = m_4 \tag{8}$$

Equations (B39) and (B42) are combined to yield

$$T_{Z,1} = \left(\frac{A_2 P_2^*}{A_4 P_4^*}\right) T_4^* \frac{h(\gamma_{P,1})}{h(\gamma_{P,4})} (1 + \varepsilon_a)(1 + \varepsilon_b) \tag{B50}$$

or

$$T_0 = \left(\frac{A_2 P_2^*}{A_4 P_4^*}\right)^2 T_4^* \frac{h(\gamma_{P,1})}{h(\gamma_4)} (1 + \varepsilon_a)(1 + \varepsilon_b)(1 + \varepsilon_c) \tag{12}$$

where

$$1 + \varepsilon_c = \frac{T_0}{T_{Z,1}} \tag{B51}$$

Above $M_1 \approx 1.4$ the entropy change $\Delta S_a$ can no longer be treated as a correction to the function $1 + \varepsilon_a$ because this entropy rise will

change the ratio $u_2/u_1$ as found from equations assuming $\Delta S_a = 0$. The velocity ratios may be found by using as end conditions the velocity ratios calculated by the formulas of reference 32 for constant specific heats:

$$\frac{u_2}{u_1} = \sqrt{\frac{\frac{\gamma - 1}{2} M_1^2 + 1}{\frac{\gamma + 1}{2} M_1^2}} \tag{B52}$$

This was done for the points calculated in figure 17, for $M_{Z,1} = 2.0$, and for the supersonic velocity ratios shown in figure 16. As is seen in figure 17 the approximation of $1 + \varepsilon_a/e^{-\Delta S_a}$ given by equation (B32) is still good.

To find $e^{-\Delta S_a/R}$ another simplifying assumption can be made for $M_1 > 1.4$. In this region almost all the entropy rise is due to the bow shock, and, thus, $\Gamma_a$ can be calculated for the normal shock alone. Also, above $M_1 = 1.4$ and when $D/u_1\tau^+ > 1.0$, $\Delta S_a \approx \Delta S_b$. For these reasons, $\varepsilon_a$ and $\varepsilon_b$ may be combined to give, for $M_1 > 1.4$:

$$\varepsilon_a + \varepsilon_b \approx \varepsilon_{a,U} + \left[1 - \frac{\Sigma_a}{(u_2/u_1)^2 - 1}\right](\varepsilon_{a,R} - \varepsilon_{a,U}) + \varepsilon_{b,U} + \left(1 - \Sigma_b^2 - \Gamma_{b,\text{subsonic}}\right)(\varepsilon_{b,R} - \varepsilon_{b,U}) \tag{B53}$$

This approximate formula seems to be good in the region $1.4 < M_1 < 2.0$.

## APPENDIX C

### SAMPLE CALCULATION FOR FIGURE 14

Given $\theta_1 = 1500^\circ$ K, $P_1 = 1$ atmosphere, $M_{Z,1} = 0.7$, gas constituents of 13.6 percent carbon dioxide, 13.8 percent water, and 72.6 percent nitrogen, a probe diameter of 1.27 centimeters (1/2 in.), and $\theta_B < 500^\circ$ K.

First, it is necessary to estimate the value of $D/u_1\tau^+$ of all the gas constituents so as to decide which vibrational modes are to be considered relaxed, partially relaxed, and unrelaxed.

Adding the specific heat by using the percentage composition and the values given in table I gives

$$c_1/R = 4.760,\ \gamma_1 = 1.2650,\ c_4/R = 3.797, \text{ and } \gamma_4 \approx 1.386$$

$$u_1 \approx M_{Z,1}\sqrt{\gamma_{Z,1}R\theta_1} = 7.4\times10^4 \text{ cm/sec}$$

Dividing the relaxation times in figure 5 by the proper partial pressures gives:

$$\tau_{N_2\text{-}N_2} = 340\times10^{-6} \text{ sec} \quad \text{(using eq. (40))}$$

$$\tau_{N_2\text{-}H_2O} \approx 36\times10^{-6} \text{ sec} \quad \text{(using eq. (41))}$$

$$\therefore \tau_{N_2} \approx 33\times10^{-6} \text{ sec} \quad \text{(using eq. (42))}$$

$$\tau_{CO_2\text{-}CO_2} \approx 0.29\times10^{-6} \text{ sec} \quad \text{(using eq. (40))}$$

$$\tau_{CO_2\text{-}H_2O} \approx 0.14\times10^{-6} \text{ sec} \quad \text{(using eq. (41))}$$

$$\therefore \tau_{CO_2} \approx 0.09\times10^{-6} \text{ sec} \quad \text{(using eq. (42))}$$

$$\tau_{H_2O} \approx 0.05\times10^{-6} \text{ sec} \quad \text{(using eq. (40))}$$

$$(D/u_1\tau^+)_{N_2} \approx 0.5$$

$$(D/u_1\tau^+)_{CO_2} \approx 190$$

$$(D/u_1\tau^+)_{H_2O} \approx 340$$

In the region $0.1 < D/u_1\tau^+ < 100$ a mode is partially relaxed. Thus, only nitrogen will be considered partially relaxed, while water and carbon dioxide will be considered fully relaxed.

Using tables I and II or equation (8) and reference 24 gives

$$\frac{c_{P,1}}{R} = 4.258, \quad \frac{c_{B,1}}{R} \approx 0.502, \quad \frac{c_{X,1}}{R} = 0$$

$$\frac{c_{P,1}\psi_P}{R} \approx 0.078, \quad \frac{c_{B,1}\psi_B}{R} \approx 0.122, \quad \frac{c_{X,1}\psi_X}{R} = 0$$

$$\frac{T_{Z,1}}{\theta_1} = 1.0760 \quad \text{(using eq. (27))}$$

$$\frac{\theta_{Z,2}}{\theta_1} \approx 0.9342 \quad \text{(using eq. (19))}$$

$$(u_{Z,2}/u_1)^2 \approx 1.945 \quad \text{(using eq. (14))}$$

$$\beta_U \approx -0.00513 \quad \text{(using eq. (20))}$$

$$\theta_{U,2}/\theta_1 \approx 0.9341 \quad \text{(using eq. (21))}$$

$$1 + \varepsilon_{a,U} \approx 1.0001 \quad \text{(using eq. (19))}$$

$$\beta_R = 0.490 \quad \text{(using eq. (23))}$$

$$\theta_{R,2}/\theta_1 \approx 0.9409 \quad \text{(using eq. (24))}$$

$$1 = \varepsilon_{a,R} = 0.9785 \quad \text{(using eq. (22))}$$

$$\beta_U^* \approx 0.0059 \quad \text{(using eq. (28))}$$

$$T_{U,2}/\theta_1 \approx 1.0759 \quad \text{(using eq. (29))}$$

$$1 + \varepsilon_{b,U} \approx 1.0000 \quad \text{(using eq. (27))}$$

$$\beta_R^* \approx 0.516 \quad \text{(using eq. (31))}$$

$$T_{R,2}/\theta_1 \approx 1.0678 \quad \text{(using eq. (32))}$$

$$1 + \varepsilon_{b,R} \approx 1.0015 \quad \text{(using eq. (30))}$$

Using the estimated value of $D/u_1\tau^+$ gives

$$(u_1/u_2)^2 \Sigma_a \approx 0.62 \quad \text{(using fig. 7)}$$

$$(u_1/u_2)^4 \Gamma_a \approx 0.06 \quad \text{(using fig. 8)}$$

$$\Sigma_b^2 \approx 0.04 \quad \text{(using fig. 9)}$$

$$\Gamma_b \approx 0.27 \quad \text{(using fig. 10)}$$

$$\varepsilon_a \approx 0.006 \quad \text{(using eq. (17))}$$

$$\varepsilon_b \approx 0.001 \quad \text{(using eq. (25))}$$

For method I:

$$\frac{T_0 - T_I}{T_0} \approx 0.007 \quad \text{(using eq. (45))}$$

For method II:

$$\frac{T_0 - T_{II}}{T_0} \approx 0.023 \quad \text{(using eqs. (33), (48), and (49))}$$

For method III:

$$\frac{T_0 - T_{III}}{T_0} \approx -0.025 \quad \text{(using eqs. (33), (51), and (52))}$$

For method IV a graph of $\gamma$ plotted against $h(\gamma)$ or the graph in figure 11 of reference 23 (where $h(\gamma) \equiv F_S(\gamma)^2$) is used.

$$\gamma_{eff} \approx 1.307 \quad \text{(using eqs. (13), (33), and (54))}$$

## REFERENCES


1. Bethe, H. E., and Teller, E.: Deviations from Thermal Equilibrium in Shock Waves. Rep. X-117, Ballistic Res. Lab., Aberdeen Proving Ground (Md.), 1945.

2. Griffith, Wayland: Vibrational Energy Lag in Shock Waves. Phys. Rev., vol. 87, no. 1, July 1, 1952, p. 234.

3. Smiley, Edward F., and Winkler, Ernst H.: Shock-Tube Measurements of Vibrational Relaxation. Jour. Chem. Phys., vol. 22, no. 12, Dec. 1954, pp. 2018-2022.

4. Blackman, Vernon: Vibrational Relaxation in Oxygen and Nitrogen. Jour. Fluid Mech., pt. 1, vol. 1, May 1956, pp. 61-85.

5. Penny, H. C., and Aroeste, H.: Vibrational Relaxation Time of Diatomic Molecules and Rocket Performance. Jour. Chem. Phys., vol. 23, no. 7, July 1955, pp. 1281-1283.

6. Kantrowitz, Arthur: Effects of Heat-Capacity Lag in Gas Dynamics. NACA WR L-457, 1944. (See also Jour. Chem. Phys., vol. 14, no. 1, Mar. 1946, pp. 150-164.)

7. Kantrowitz, Arthur, and Huber, Paul W.: Heat-Capacity Lag in Turbine-Working Fluids. NACA WR L-21, 1944. (See also Jour. Chem. Phys., vol. 15, no. 5, May 1947, pp. 275-284.)

8. Griffith, W.: Vibrational Relaxation Times in Gases. Jour. Appl. Phys., vol. 21, Dec. 1950, pp. 1319-1325.

9. Tuesday, C. S., and Boudart, M.: Vibrational Relaxation Times by the Impact Tube Method. Tech. Note 7, James Forrestal Res. Center, Princeton Univ., Jan. 1955. (Contract AF-33(038)-23976.)

10. Spooner, Robert B.: Effect of Heat-Capacity Lag on a Variety of Turbine-Nozzle Flow Processes. NACA TN 2193, 1950.

11. Walker, Richard: Heat Capacity Lag in Gases. NACA TN 2537, 1951.

12. Schwartz, R. N., Slawsky, Z. I., and Herzfeld, K. F.: Calculation of Vibrational Relaxation Times in Gases. Jour. Chem. Phys., vol. 20, Oct. 1952, pp. 1591-1599.

13. Schwartz, R. N., and Herzfeld, K. F.: Vibrational Relaxation Times in Gases (Three Dimensional Treatment). Jour. Chem. Phys., vol. 22, May 1954, pp. 767-773.

14. Brout, Robert: Thermal Relaxation in Gases. Jour. Chem. Phys., vol. 22, no. 9, Sept. 1954, pp. 1500-1502.

15. Walker, Richard A., Rossing, Thomas D., and Legvold, Sam: The Role of Triple Collisions in Excitation of Molecular Vibrations in Nitrous Oxide. NACA TN 3210, 1954.

16. Rossing, Thomas D., Amme, Robert C., and Legvold, Sam: Heat Capacity Lag in Gaseous Mixtures. NACA TN 3558, 1956.

17. Sette, D., and Hubbard, J. C.: Note on Thermal Relaxation of Carbon Dioxide in Presence of Water and $D_2O$ Molecules. Jour. Acoustical Soc. Am., vol. 25, Sept. 1953, pp. 994-997.

18. Herzfeld, Karl F.: Relaxation Phenomena in Gases. Vol. I of High Speed Aerodynamics and Jet Propulsion - Thermodynamics and Physics of Matter, sec. H, ch. 1, Frederick D. Rossini, ed., Princeton Univ. Press, 1955, pp. 646-735.

19. Moore, David William, Jr.: A Pneumatic Method for Measuring High-Temperature Gases. Aero. Eng. Rev., vol. 7, no. 5, May 1948, pp. 30-34.

20. Wildhack, W. A.: A Versatile Pneumatic Instrument Based on Critical Flow. Rev. Sci. Inst., vol. 21, no. 1, 1950, pp. 25-30.

21. Blackshear, Perry L., Jr.: Sonic-Flow-Orifice Temperature Probe for High-Gas-Temperature Measurements. NACA TN 2167, 1950.

22. Bundy, F. P., and Strong, H. M.: Measurement of Flame Temperature, Pressure and Velocity. Vol. IX of High Speed Aerodynamics and Jet Propulsion - Physical Measurements in Gas Dynamics and Combustion, sec. I, pt. 2, H. S. Taylor, et al., eds., Princeton Univ. Press, 1954, pp. 343-386.

23. Simmons, Frederick S., and Glawe, George E.: Theory and Design of a Pneumatic Temperature Probe and Experimental Results Obtained in a High-Temperature Gas Stream. NACA TN 3893, 1957.

24. Hilsenrath, Joseph, et al.: Tables of Thermal Properties of Gases. Circular 564, U.S. Dept. Commerce, NBS, Nov. 1, 1955.

25. Fehling, H. R., and Leser, T.: Determination of the True Composition of the Products of the Theoretical Combustion with Oxygen and Oxygen/Nitrogen Mixtures at Temperatures up to 2500° C at Atmospheric Pressures. Third Symposium on Combustion and Flame and Explosion Phenomena, The Williams & Wilkins Co., 1949, pp. 634-640.

26. Huff, Vearl N., and Calvert, Clyde S.: Charts for the Computation of Equilibrium Composition of Chemical Reactions in the Carbon-Oxygen-Nitrogen System at Temperatures from 2000° to 5000° K. NACA TN 1653, 1948.

27. Lewis, Bernard, and Von Elbe, Guenther: Combustion, Flames and Explosions of Gases. Cambridge Univ. Press, 1938.

28. Gilmore, F. R.: Equilibrium Composition and Thermodynamic Properties of Air to 24,000° K. Rep. 1543, Rand Corp., Aug. 24, 1955.

29. Woolley, Harold W.: Effect of Dissociation on Thermodynamic Properties of Pure Diatomic Gases. NACA TN 3270, 1955.

30. Hilsenrath, Joseph, and Beckett, Charles W.: Thermodynamic Properties of Argon-Free Air ($0.78847N_2$, $0.211530_2$) to 15,000° K. Rep. 3991, U.S. Dept. Commerce, NBS, Apr. 1, 1955.

31. Evans, John S.: Method for Calculating Effects of Dissociation on Flow Variables in the Relaxation Zone Behind Normal Shock Waves. NACA TN 3860, 1956.

32. Ames Research Staff: Equations, Tables, and Charts for Compressible Flow. NACA Rep. 1135, 1953. (Supersedes NACA TN 1428.)

33. Kennard, Earle H.: Kinetic Theory of Gases. McGraw-Hill Book Co., Inc., 1938.

34. Landau, L., und Teller, E.: Zur Theorie der Schalldispersion. Phys. Zs. d. Sowjetunion, Bd. 10, Heft 1, 1936, pp. 34-43.

35. Moeckel, W. E.: Approximate Method for Predicting Form and Location of Detached Shock Waves Ahead of Plane or Axially Symmetric Bodies. NACA TN 1921, 1949.

TABLE I. - TRANSLATIONAL PLUS ROTATIONAL AND VIBRATIONAL VALUES OF SPECIFIC HEATS FOR DIFFERENT PURE GASES (IDEAL GAS VALUES)

[Data obtained from ref. 24.]

| Mode | Temperature, °K | c/R (a) | | | | |
|---|---|---|---|---|---|---|
| | | Carbon dioxide | Water | Nitrogen | Oxygen | Carbon monoxide |
| Translational plus rotational | All temperatures | 3.5000 | 4.0000 | 3.5000 | 3.5000 | 3.5000 |
| Vibrational | 500 | 1.8671 | 0.2345 | 0.0578 | 0.2396 | 0.083 |
| Vibrational | 1000 | 3.0318 | 0.9569 | 0.4326 | 0.6958 | 0.491 |
| Vibrational | 1500 | 3.521 | 1.6526 | 0.6919 | 0.8975 | 0.736 |
| Vibrational | 2000 | 3.758 | 2.1460 | 0.8268 | 1.0436 | 0.859 |
| Vibrational | 2500 | 3.893 | 2.4727 | 0.9047 | 1.1808 | 0.929 |
| Vibrational | 3000 | 3.984 | 2.6945 | 0.9545 | 1.3062 | 0.976 |

| Temperature, °K | c/R for air (a) | | | |
|---|---|---|---|---|
| | All translational and rotational modes | All vibrational modes | All modes except nitrogen vibrational modes | Nitrogen vibrational modes |
| 500 | 3.4906 | 0.0959 | 3.5414 | 0.0451 |
| 1000 | 3.4906 | 0.5044 | 3.6374 | 0.3376 |
| 1500 | 3.4906 | 0.7287 | 3.6802 | 0.5391 |
| 2000 | 3.4906 | 0.8855 | 3.7109 | 0.6452 |
| 2500 | 3.4906 | 0.9550 | 3.7397 | 0.7059 |
| 3000 | 3.4906 | 1.0203 | 3.7660 | 0.7448 |

(a) $c = \left(\frac{\partial E}{\partial \theta}\right)_p$.

TABLE II. - VALUES OF SPECIFIC-HEAT FUNCTION (IDEAL GAS)

| Mode | Temperature, °K | $\Psi$ (a) | | | | |
|---|---|---|---|---|---|---|
| | | Carbon dioxide | Water | Nitrogen | Oxygen | Carbon monoxide |
| Translational plus rotational | All temperatures | 0 | 0 | 0 | 0 | 0 |
| Vibrational | 1500 | 0.140 | 0.544 | 0.402 | 0.328 | 0.346 |
| Vibrational | 2000 | 0.093 | 0.299 | 0.243 | 0.270 | 0.209 |
| Vibrational | 2500 | 0.069 | 0.270 | 0.169 | 0.281 | 0.151 |
| Vibrational | 3000 | 0.058 | 0.206 | 0.129 | 0.267 | 0.123 |

| Temperature, °K | $\Psi$ for air (a) | | | |
|---|---|---|---|---|
| | All translational and rotational modes | All vibrational modes | All modes except nitrogen vibrational modes | Nitrogen vibrational modes |
| 1500 | 0 | 0.368 | 0.020 | 0.402 |
| 2000 | 0 | 0.298 | 0.020 | 0.243 |
| 2500 | 0 | 0.198 | 0.022 | 0.169 |
| 3000 | 0 | 0.193 | 0.024 | 0.129 |

[a] $\Psi = \frac{1}{2}\left(\frac{\partial c}{d\theta}\right)\left(\frac{\theta_1}{c_1}\right)$.

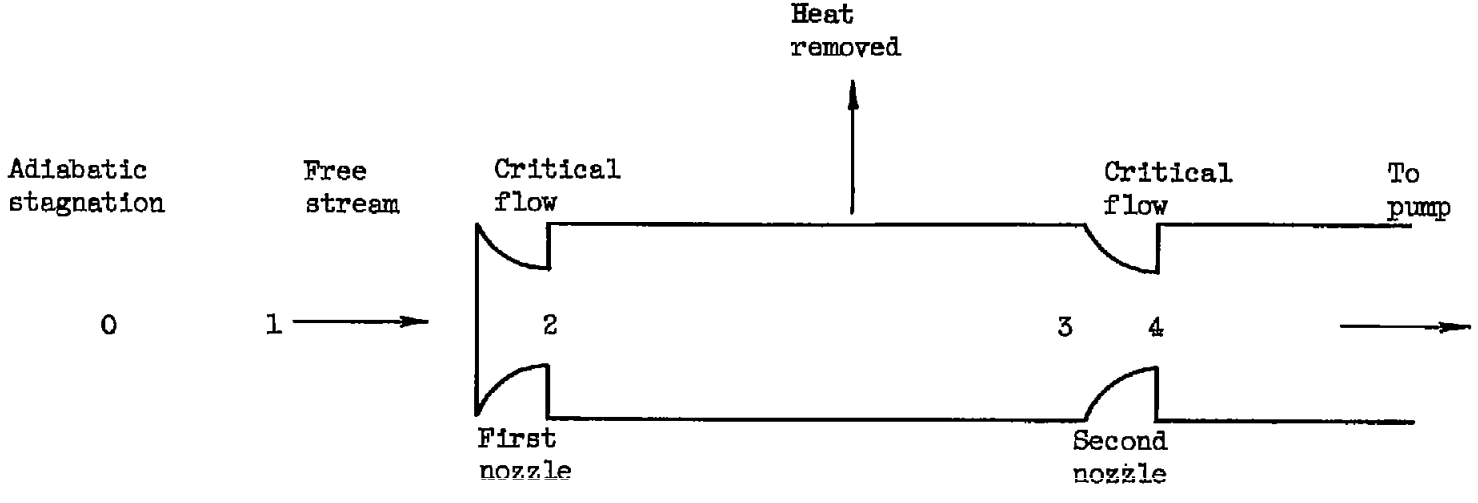


Figure 1. - Schematic diagram of pneumatic probe showing stations.

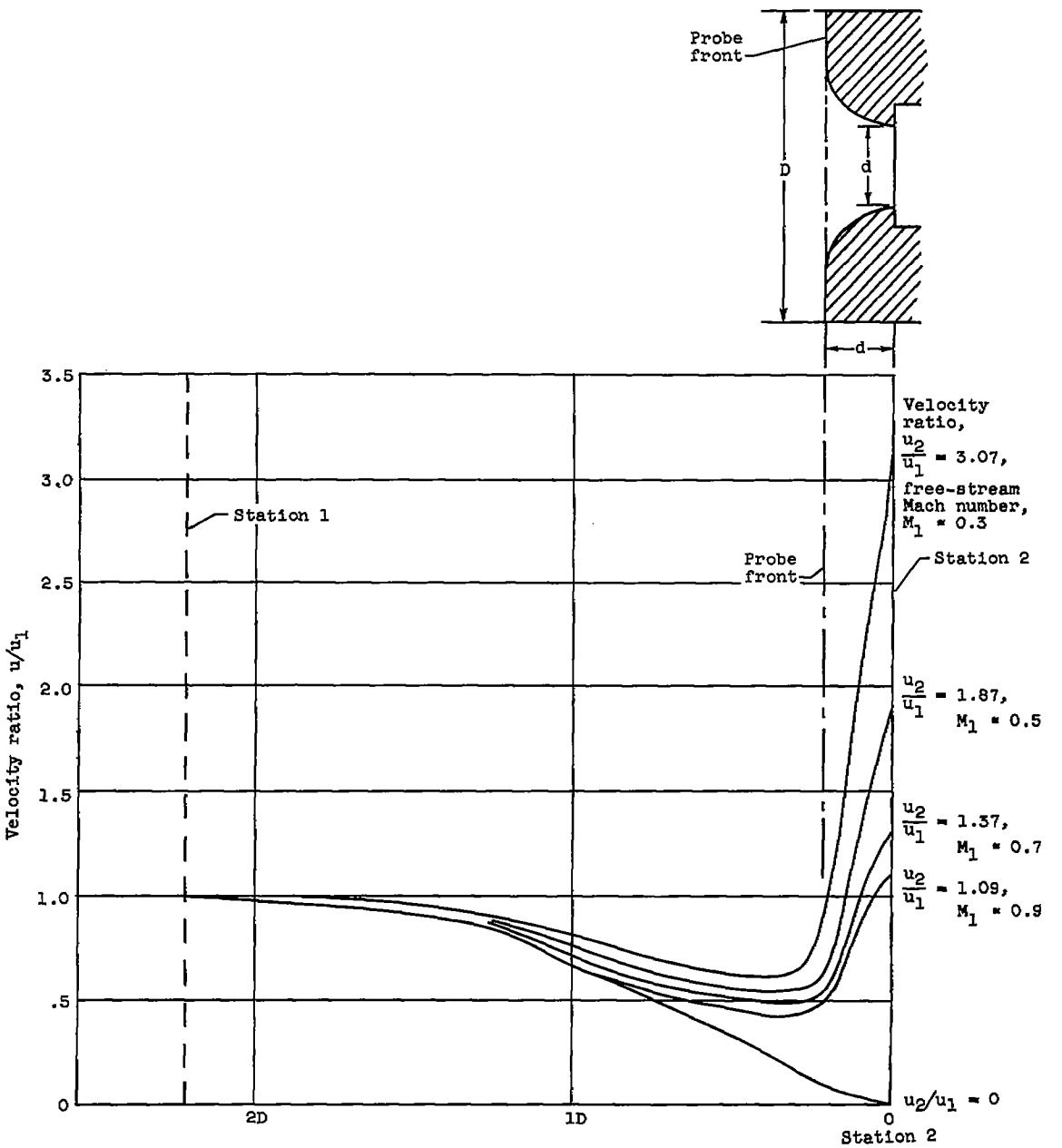


Distance from point of critical velocity (station 2), probe diam., D

Figure 2. - Probe shape and experimentally obtained velocity profiles.

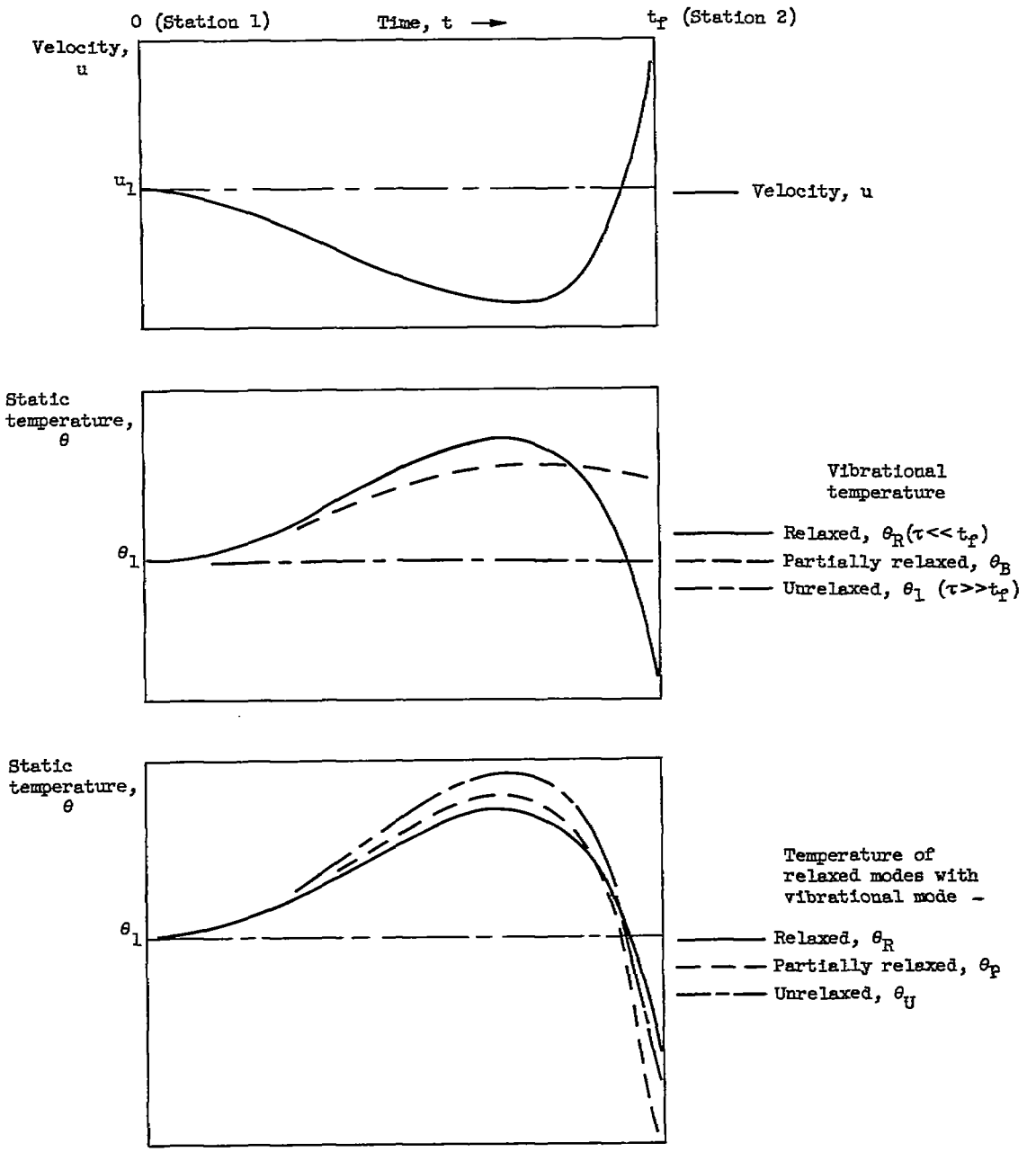


Figure 3. - Schematic diagram showing effects of relaxation on temperature.

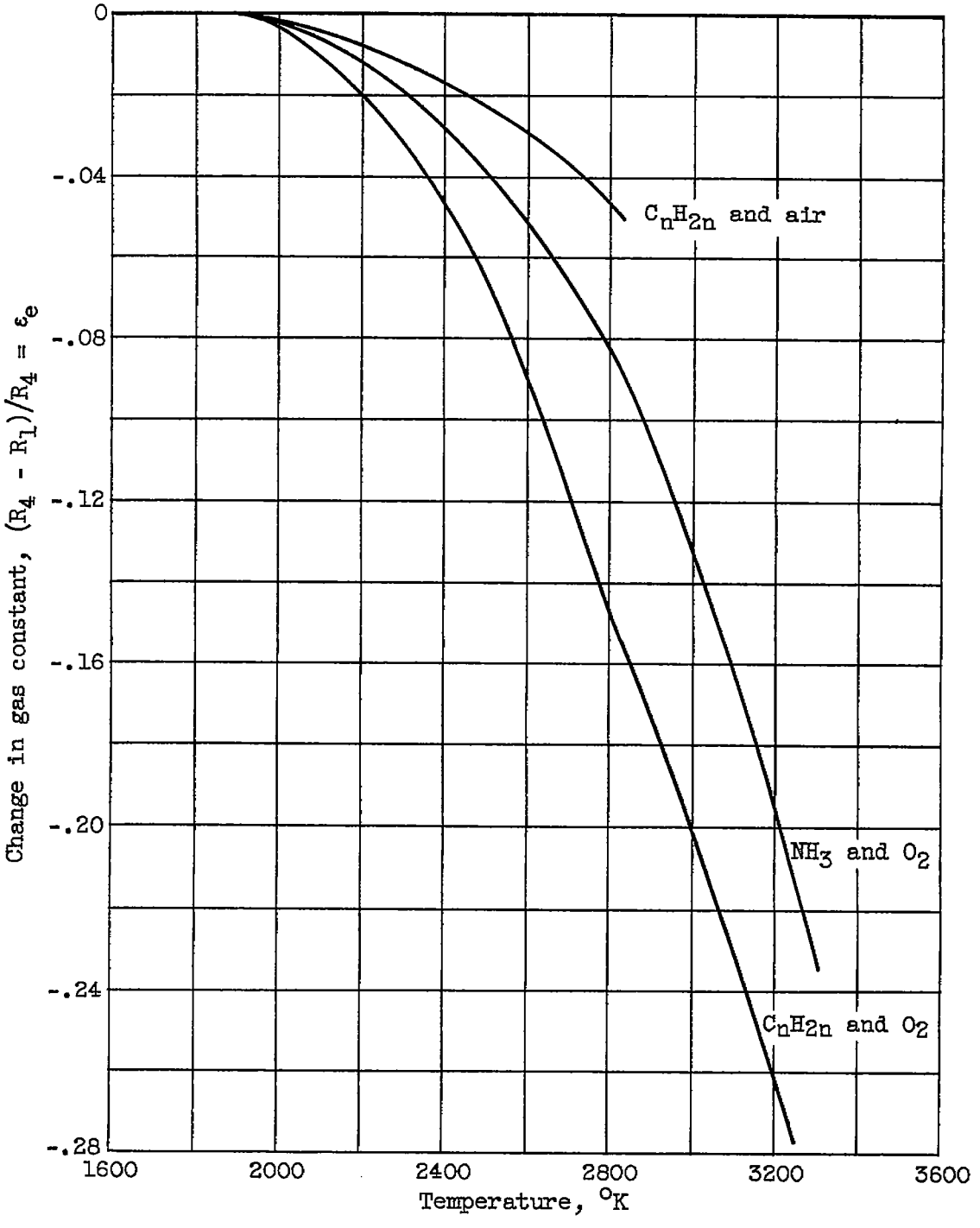


Figure 4. - Effect of dissociation on variation of gas constant with temperature for three combustion processes at atmospheric pressure.

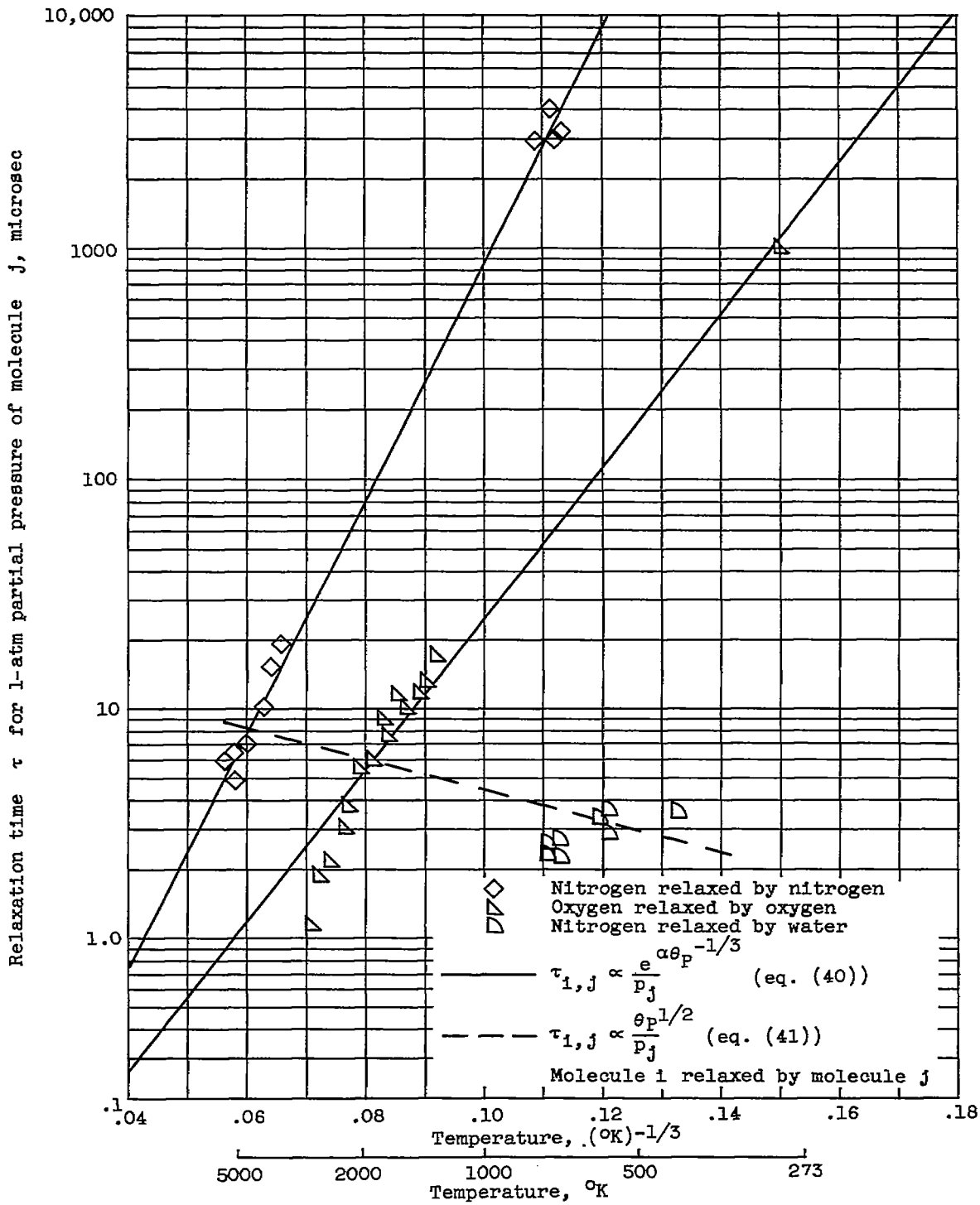


(a) Nitrogen, oxygen, and water.

Figure 5. - Experimental relaxation times as functions of temperature.

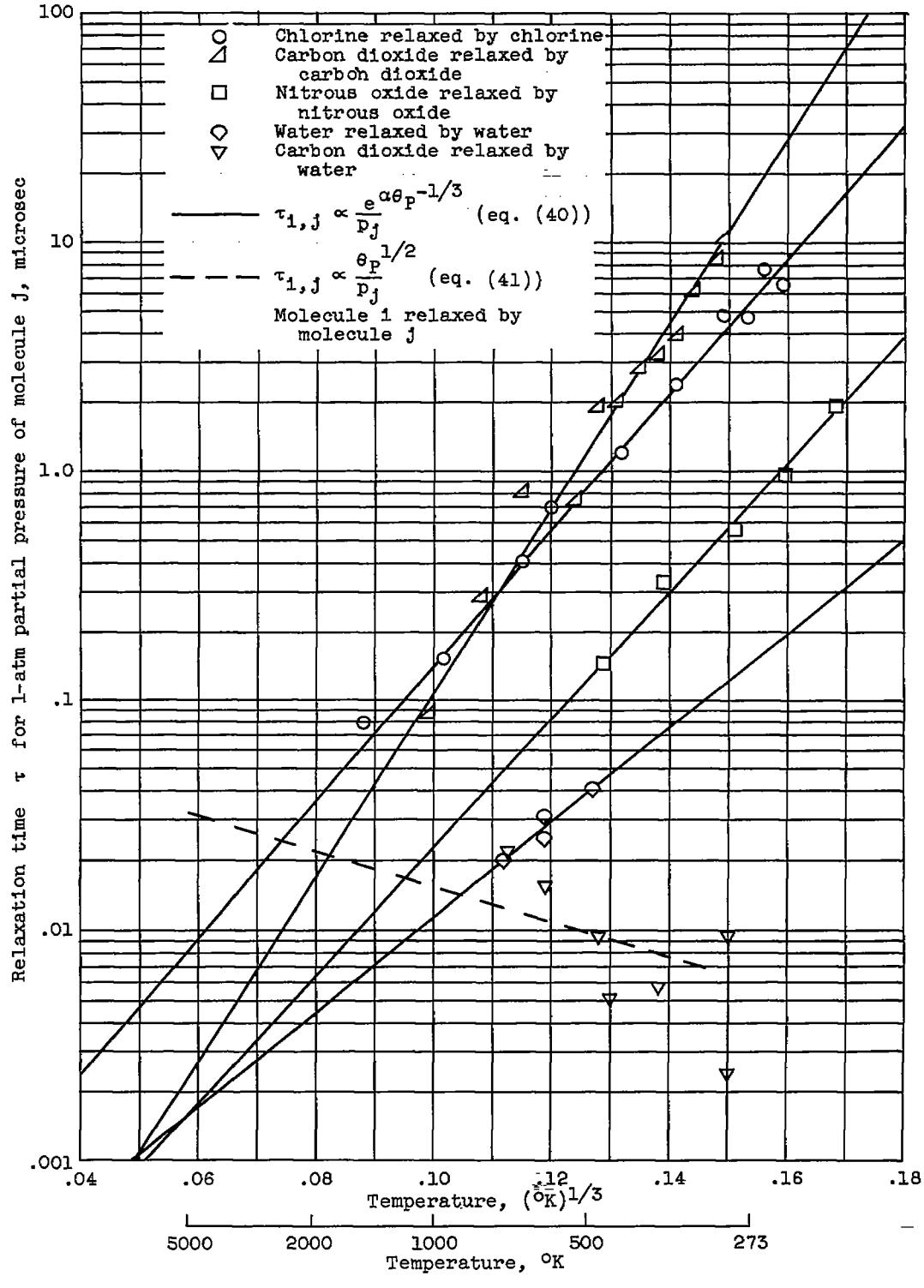


(b) Chlorine, carbon dioxide, nitrous oxide, and water.

Figure 5. - Concluded. Experimental relaxation times as functions of temperature.

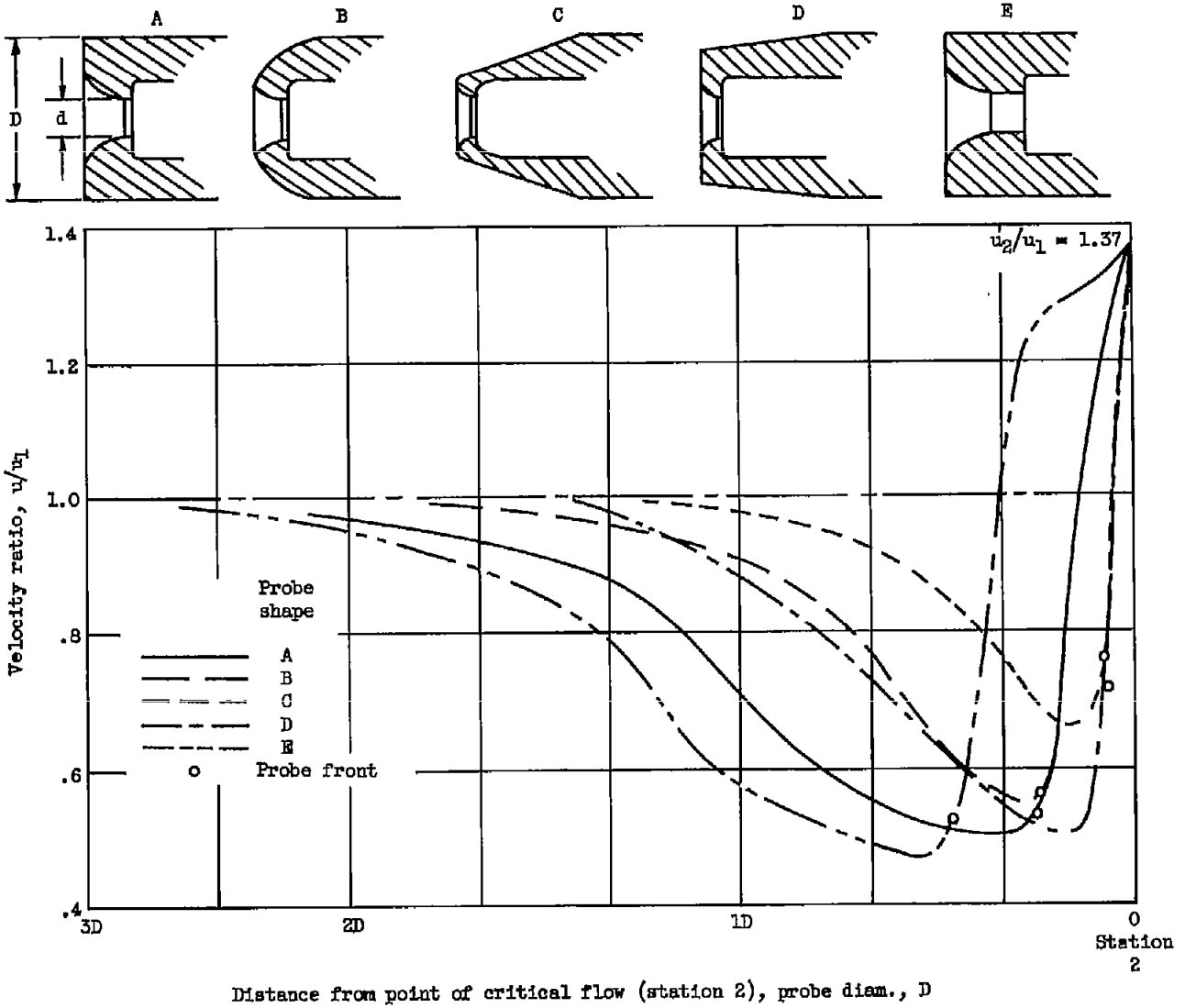


Figure 6. - Velocity profiles of five probe shapes. Free-stream Mach number, ≈ 0.7; d/D = 1/4.

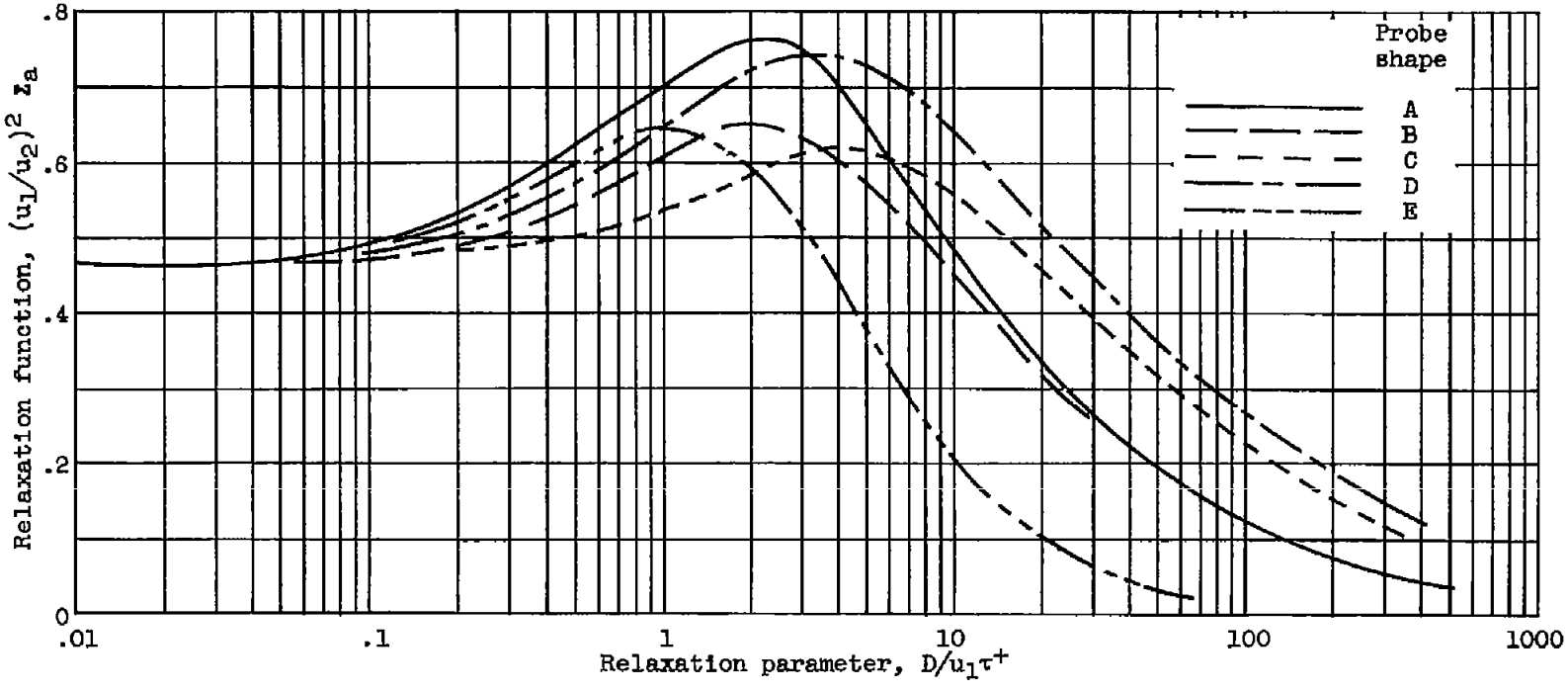


Figure 7. - Variation of relaxation function $\Sigma_a$ with relaxation parameter for five probe shapes shown in figure 6. Free-stream Mach number, = 0.7; velocity ratio, 1.37.

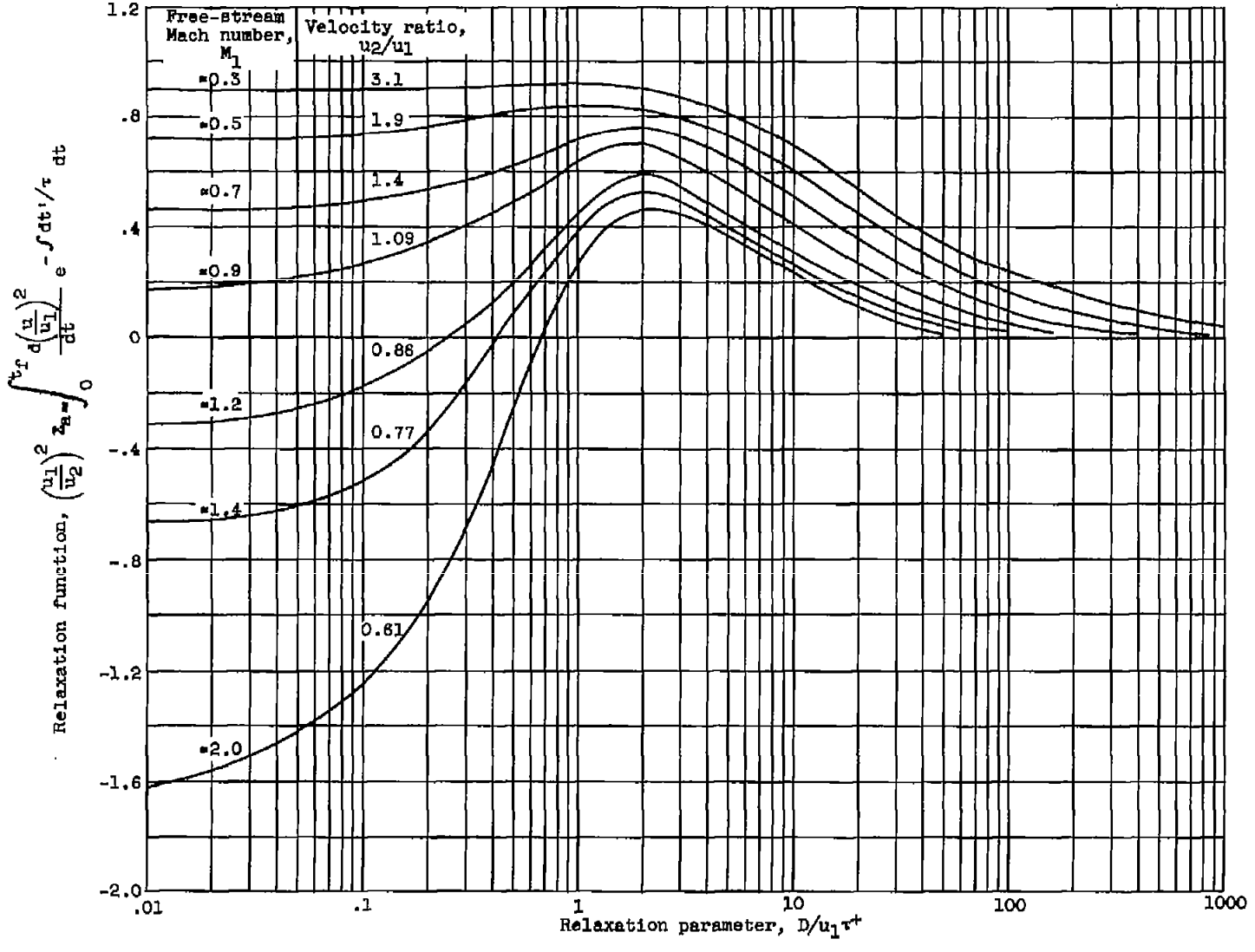


Figure 8. - Variation of relaxation function $Z_a$ with velocity ratio and relaxation parameter. Typical probe shape (probe A of fig. 6 or probe of fig. 2).

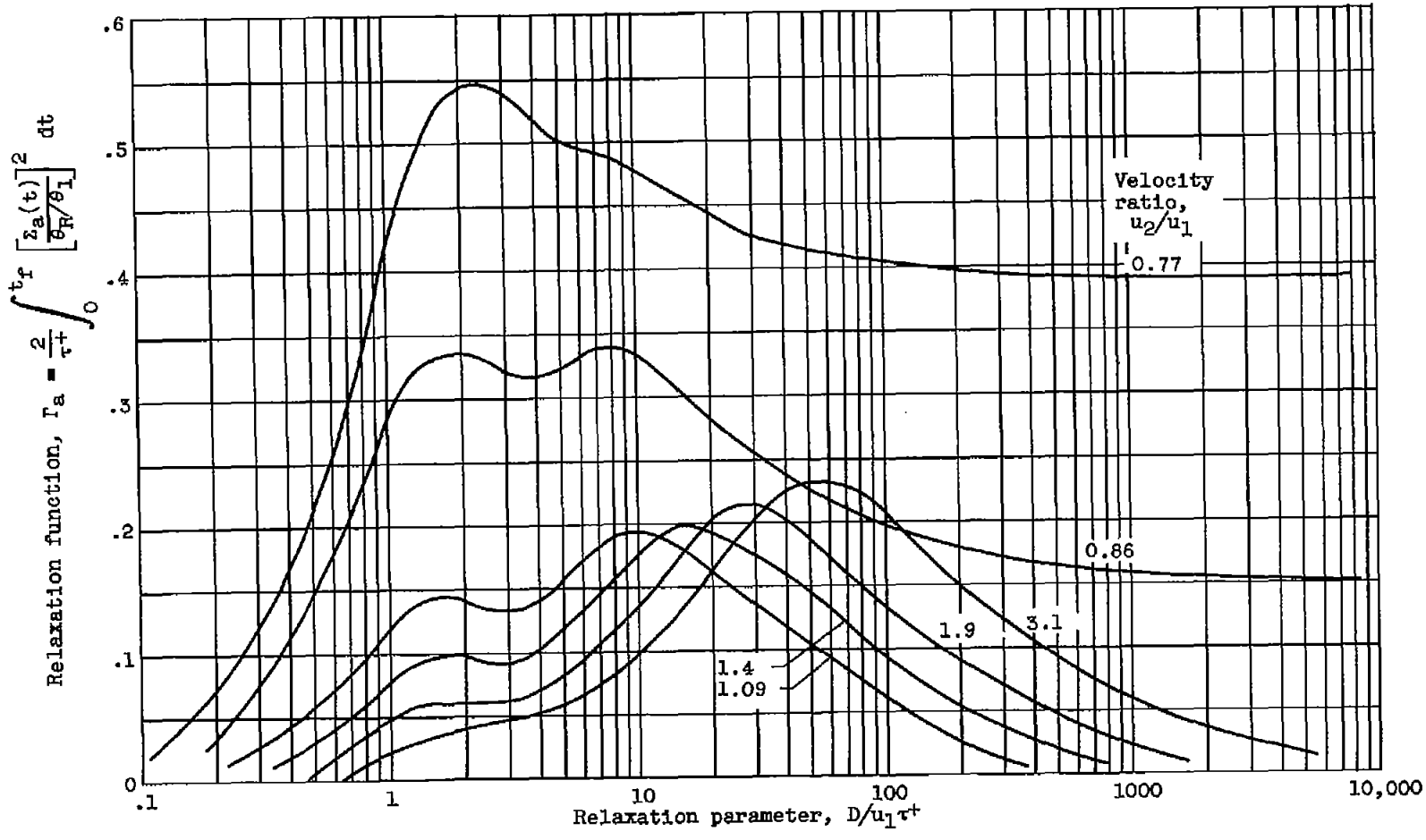


Figure 9. - Variation of relaxation function $\Gamma_a$ with velocity ratio and relaxation parameter. Typical probe shape (probe A of fig. 6 or probe shape of fig. 2); 0.3 < Mach number < 1.4.

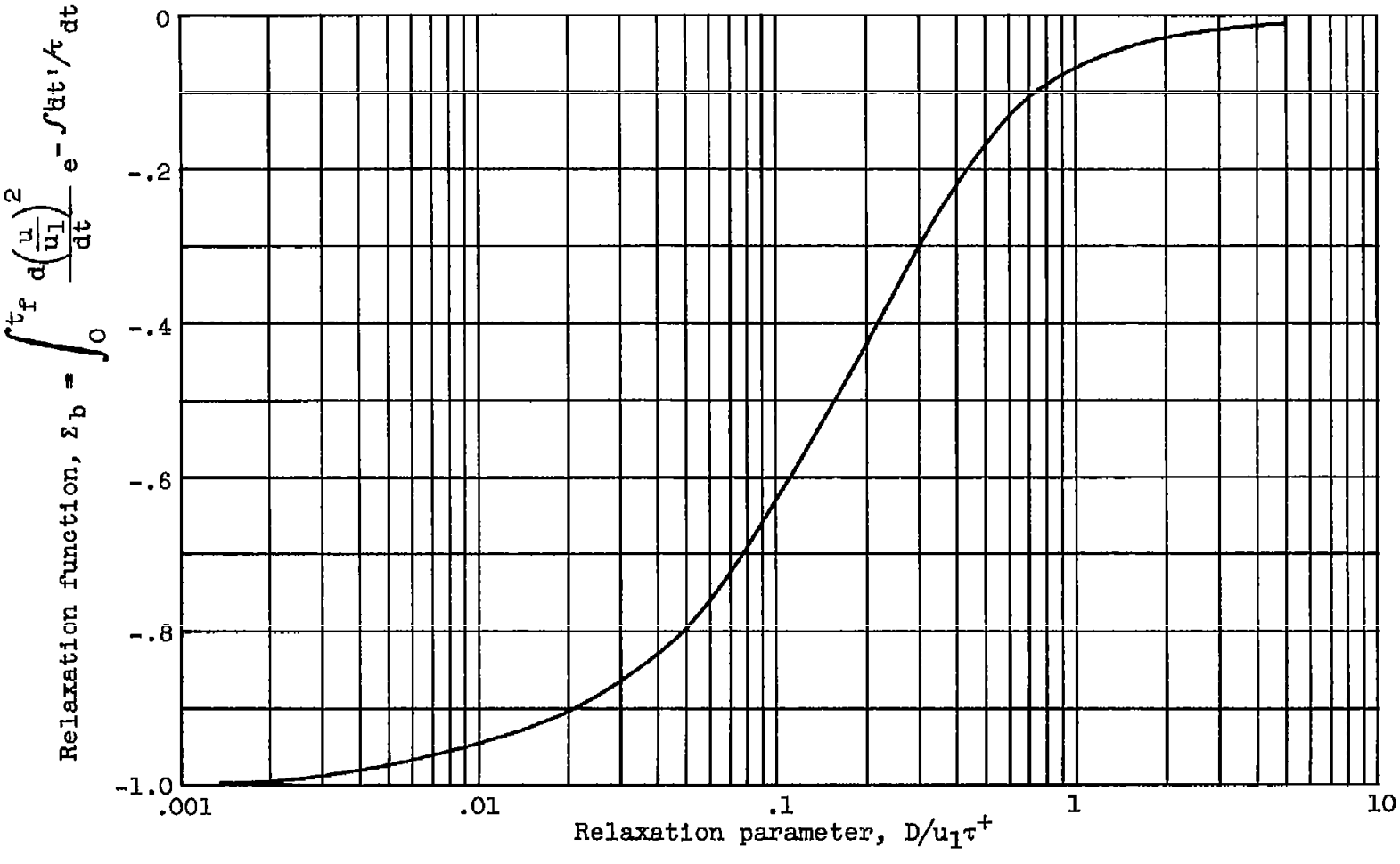


Figure 10. - Variation of relaxation function $\Sigma_b$ with relaxation parameter. Typical probe shape (probe A of fig. 6 or probe shape of fig. 2); 0.3 < Mach number < 2.0.

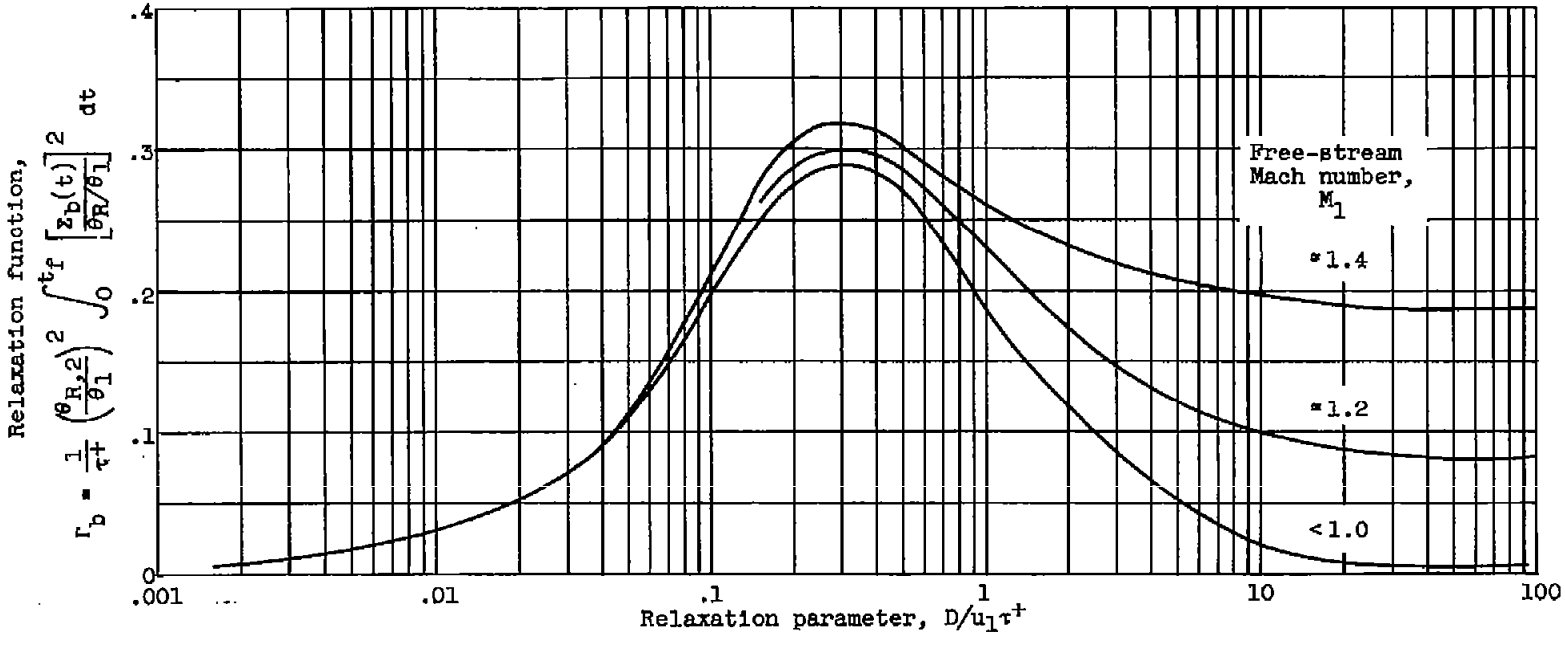


Figure 11. - Variation of relaxation function $\Gamma_b$ with free-stream Mach number and relaxation parameter. Typical probe shape (probe A of fig. 6 or probe shape of fig. 2); 0.3 < Mach number < 1.4.

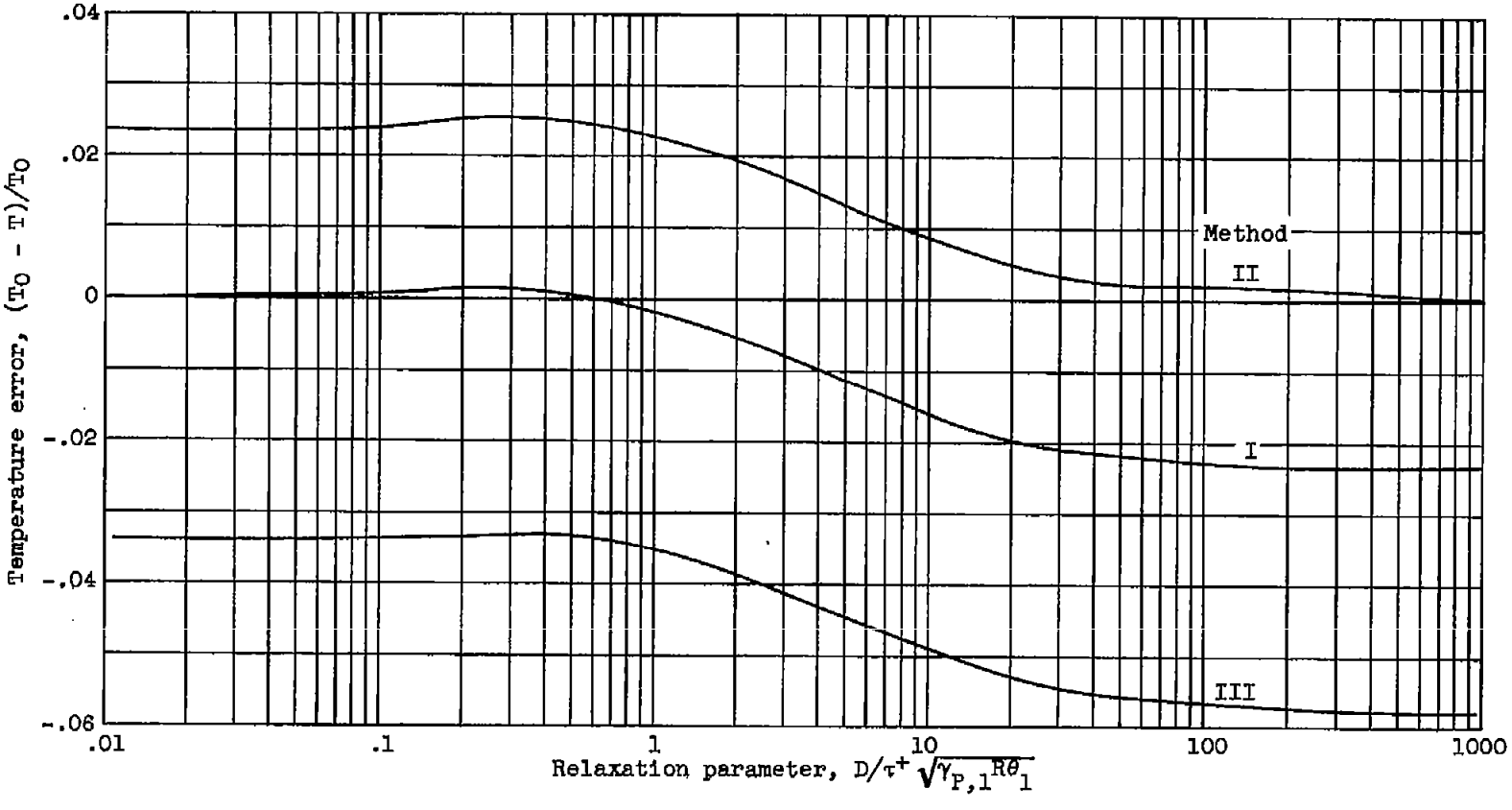


(a) Mach number, = 0.3.

Figure 12. - Variation of temperature error with relaxation parameter for three methods of calculation. $\gamma_{P,1} = 1.333$; $\gamma_1 = 1.285$; $\gamma_4 = 1.400$; $\psi_P = \psi_B = 0$.

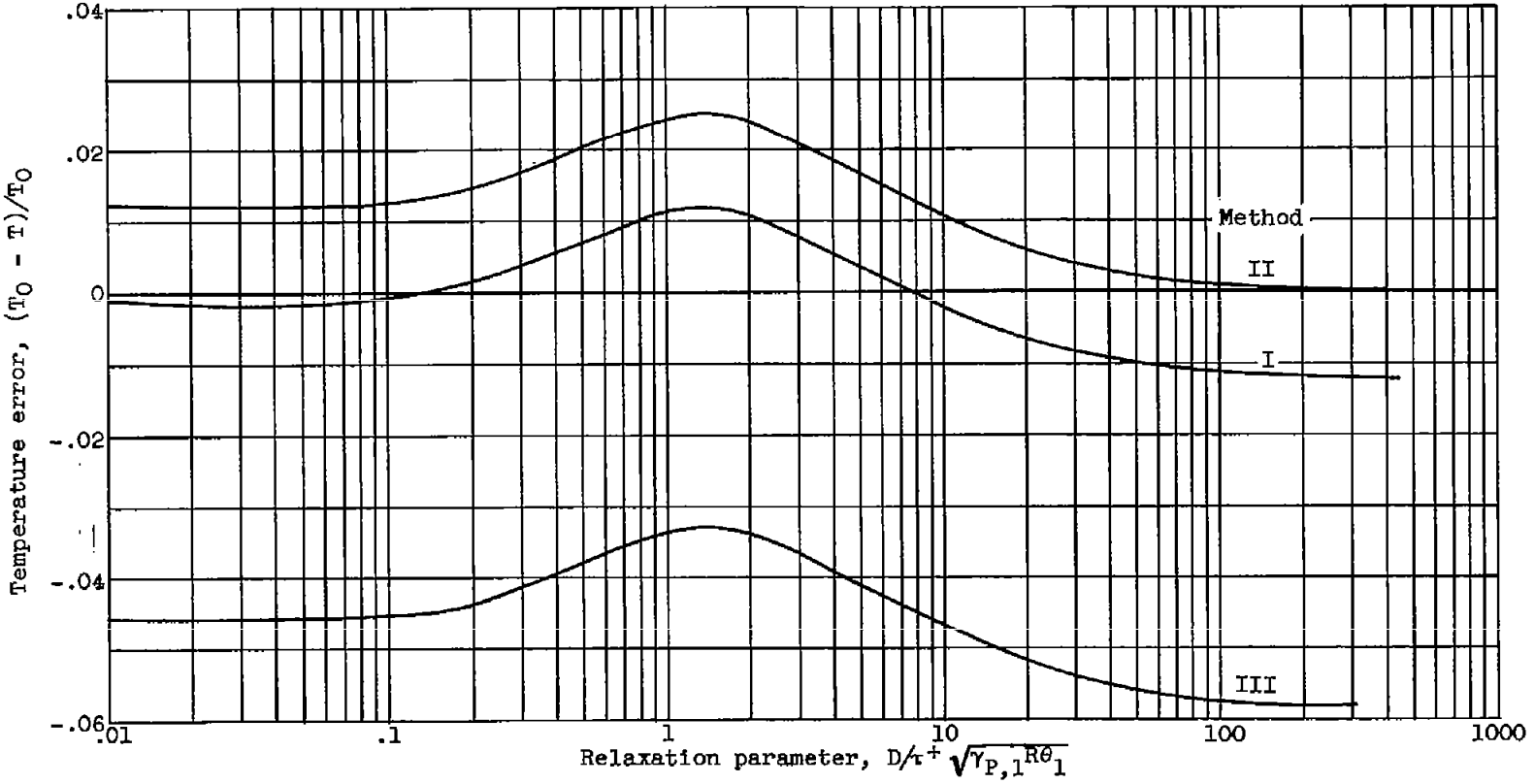


(b) Mach number, ∞0.9.

Figure 12. - Continued. Variation of temperature error with relaxation parameter for three methods of calculation. $\gamma_{P,1} = 1.333$; $\gamma_1 = 1.285$; $\gamma_4 = 1.400$; $\psi_P = \psi_B = 0$.

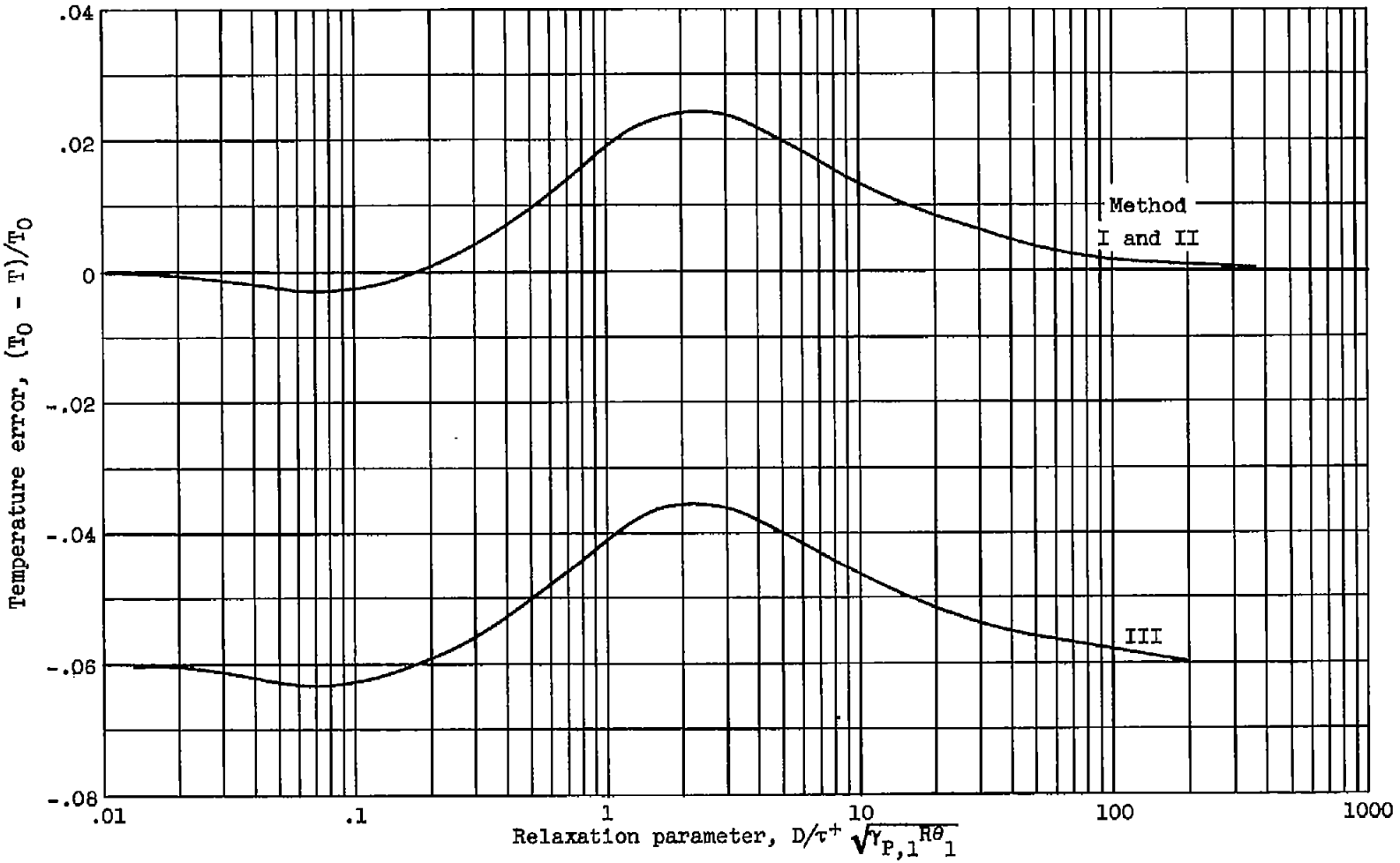


(c) Mach number, 1.4.

Figure 12. - Concluded. Variation of temperature error with relaxation parameter for three methods of calculation. $\gamma_{P,1} = 1.333$; $\gamma_1 = 1.285$; $\gamma_4 = 1.400$; $\psi_P = \psi_B = 0$.

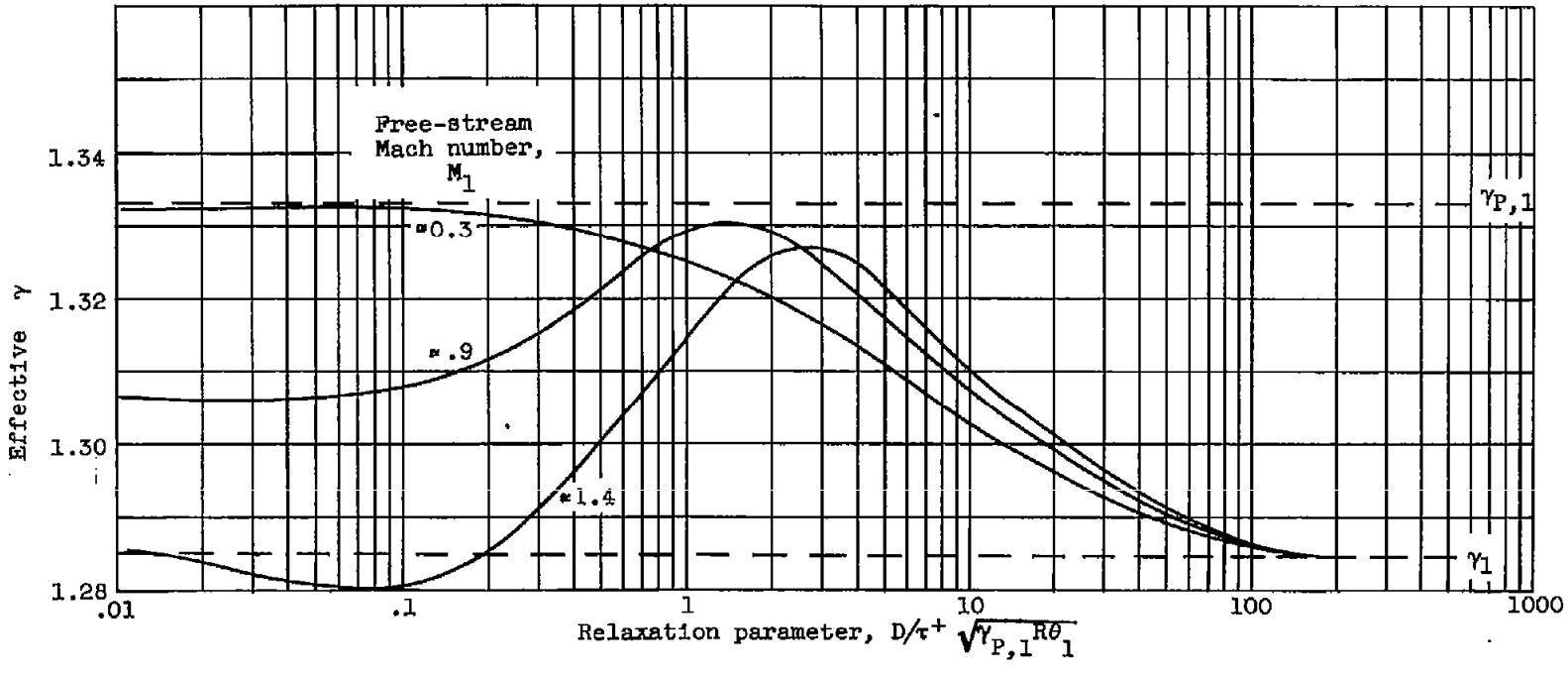


Figure 13. - Variation of effective $\gamma$ of method IV for three Mach numbers as function of relaxation parameter. $\gamma_{P,1} = 1.333$; $\gamma_1 = 1.285$; $\gamma_4 = 1.400$; $\psi_P = \psi_B = 0$.

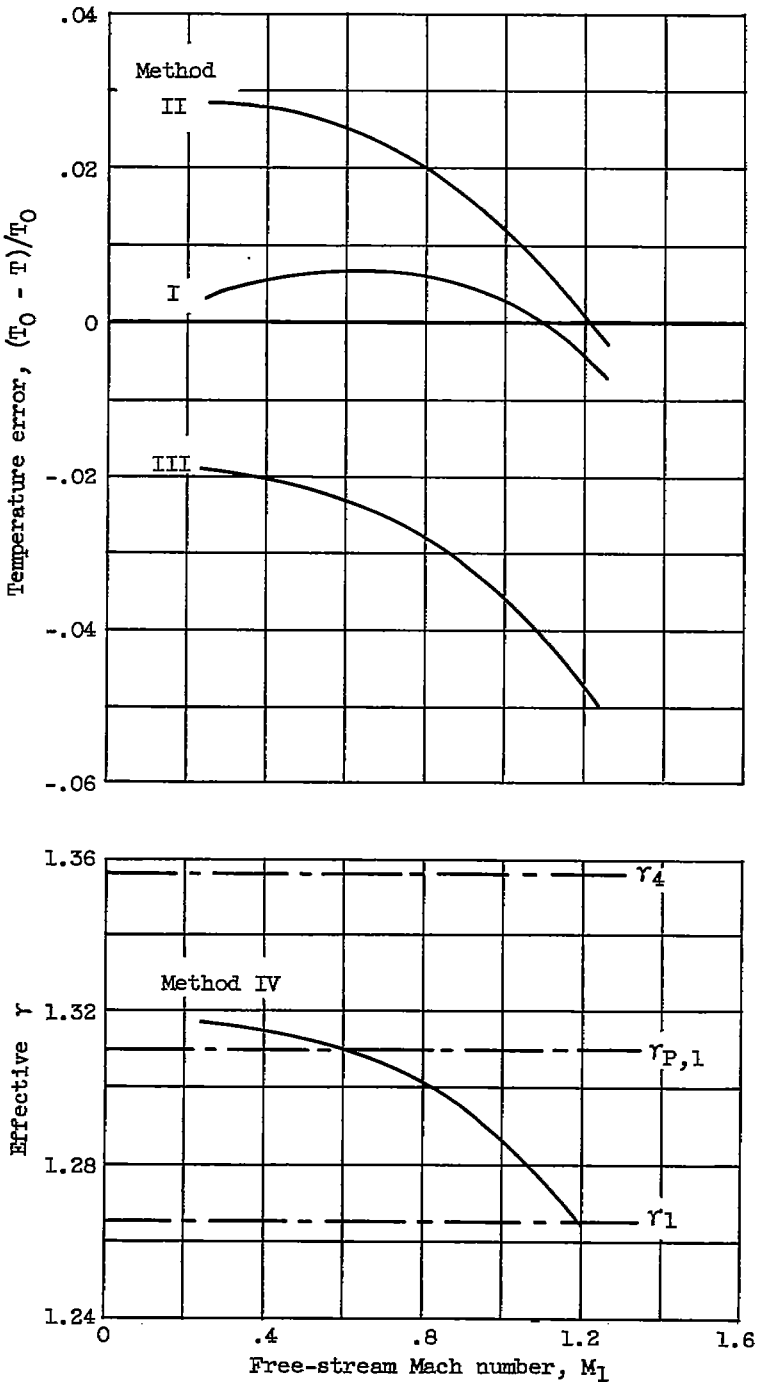


Figure 14. - Temperature error and effective $\gamma$ using the four methods for a gas composed of combustion products of heavy hydrocarbon and air. Static free-stream temperature, 1500° K; static free-stream pressure, 1 atmosphere.

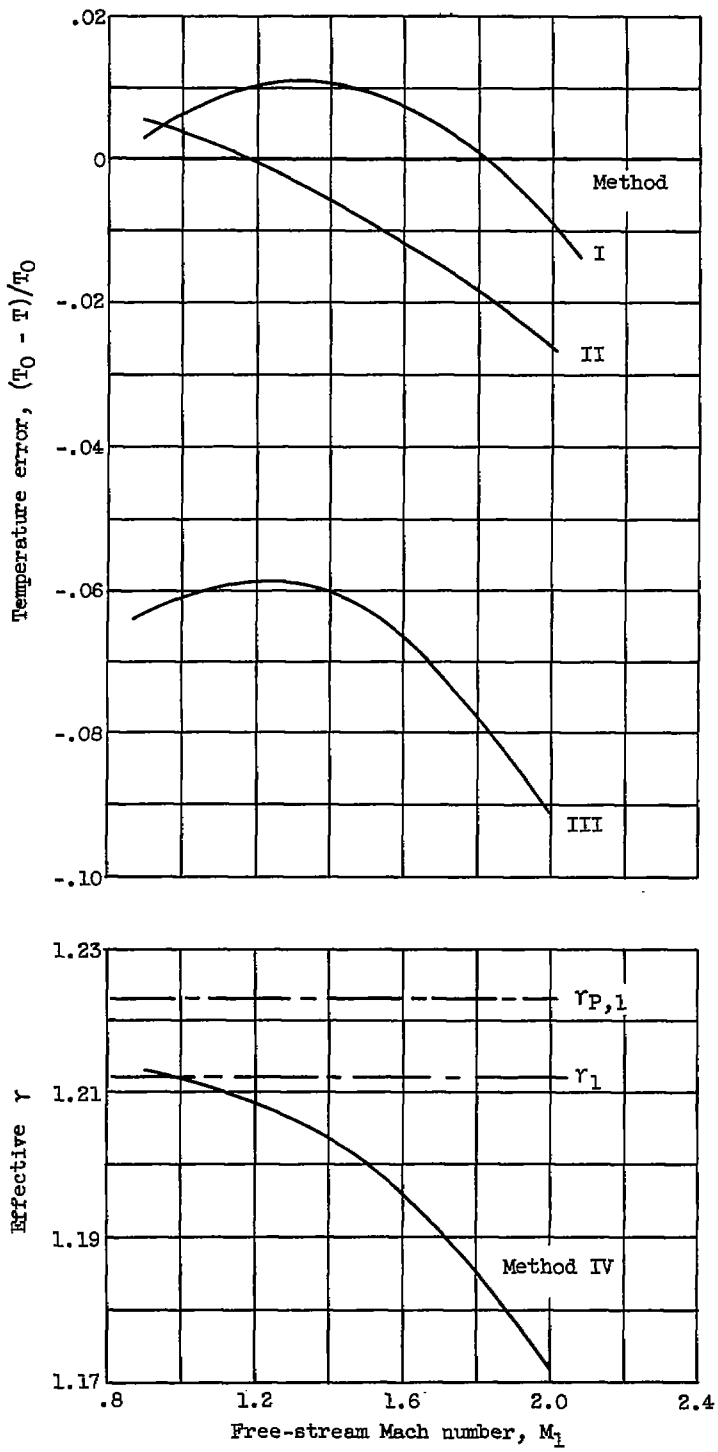


Figure 15. - Variation of temperature error and effective $\gamma$ with free-stream Mach number for gas composed of combustion products of ammonia and oxygen at 1-atmosphere pressure. Static temperature, 2000° K; static temperature at station 4, ≃500° K.

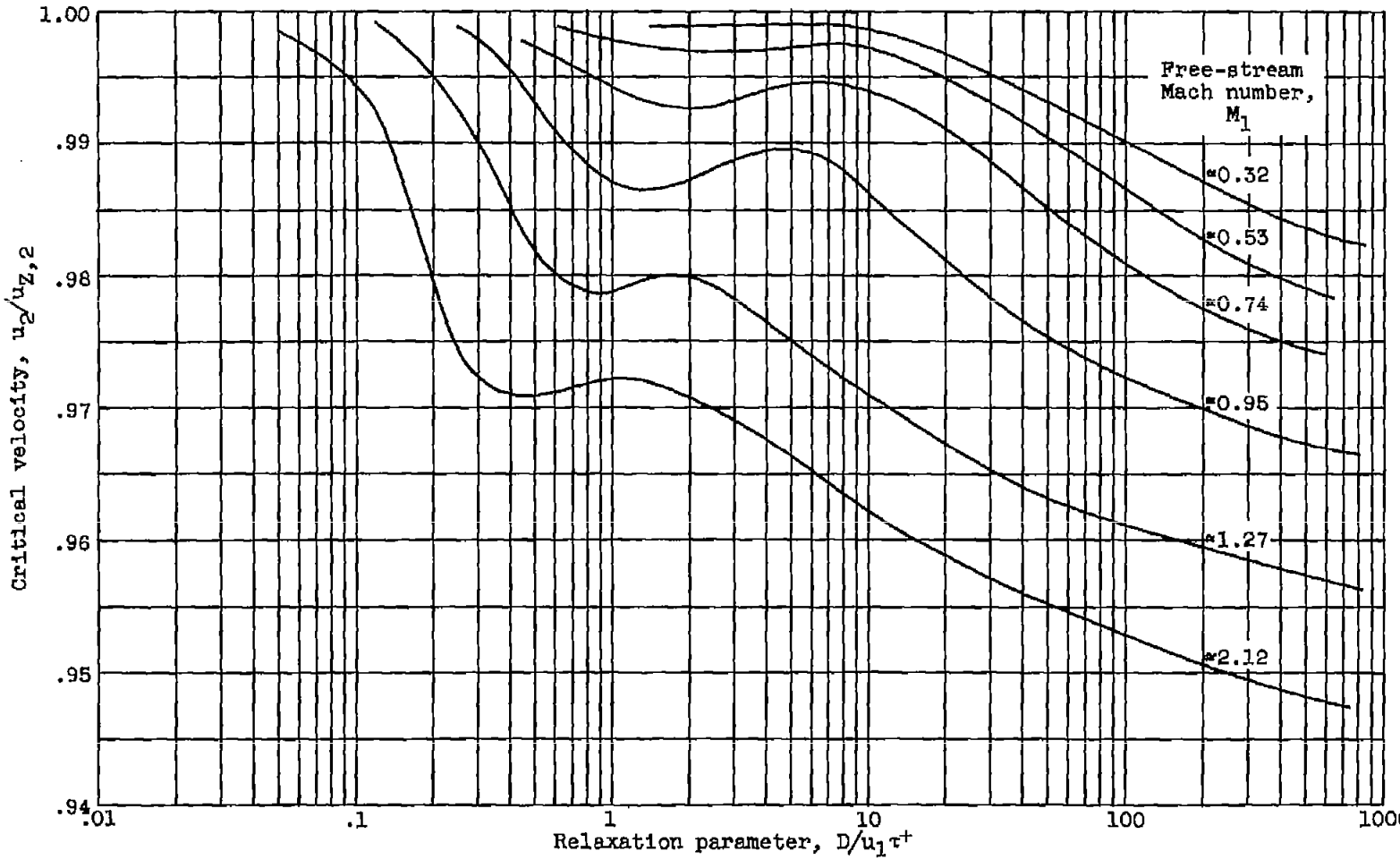


Figure 16. - Variation of critical velocity with relaxation parameter and free-stream Mach number. $c_{p,1} = 3.5R$; $c_1 = 4.5R$; $c_{B,1} = 1.0R$; $\psi_p = \psi = \psi_B = 0$.

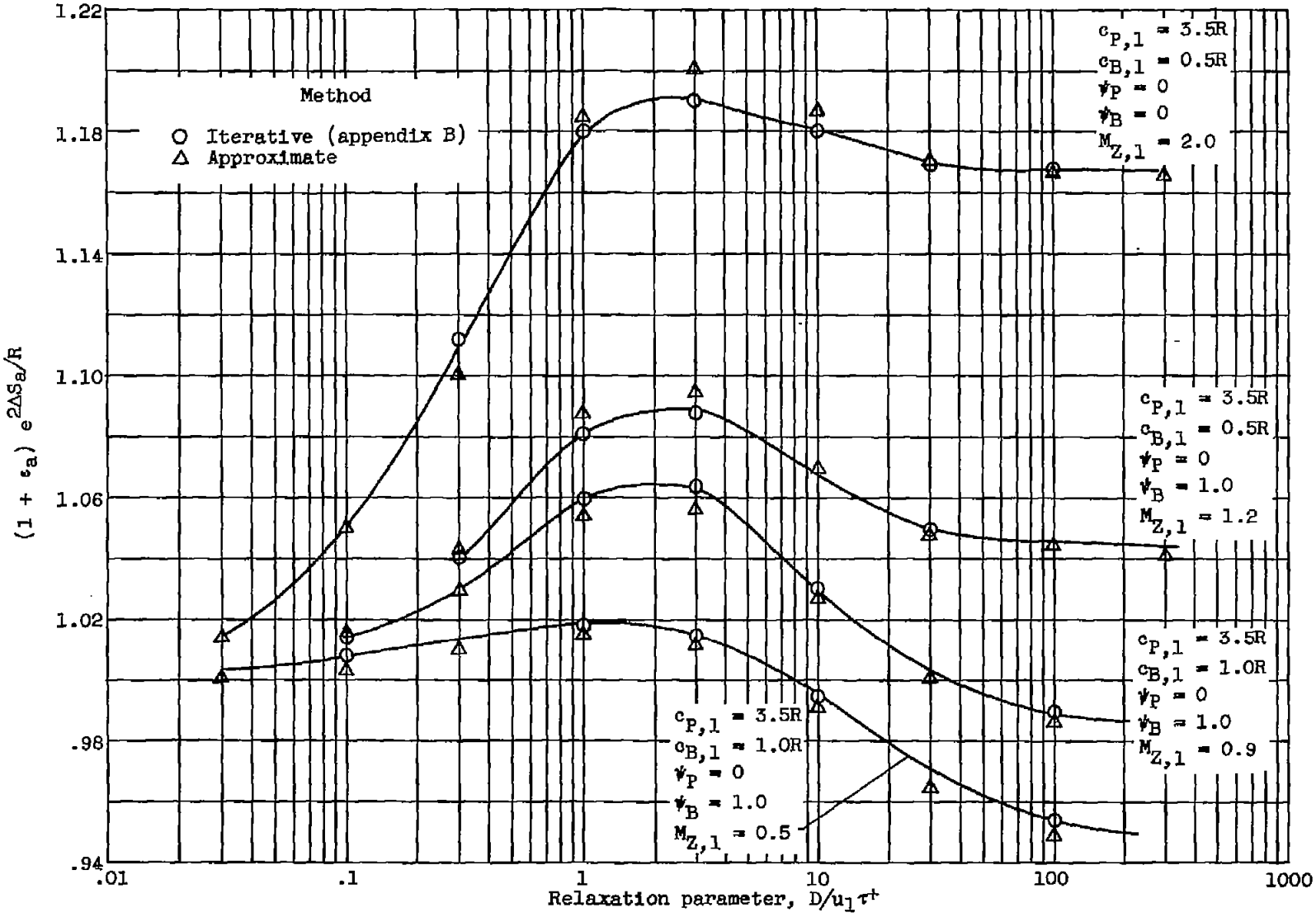


Figure 17. - Comparison of calculations of $(1 + \epsilon_a)\ e^{2\Delta S_a/R}$.

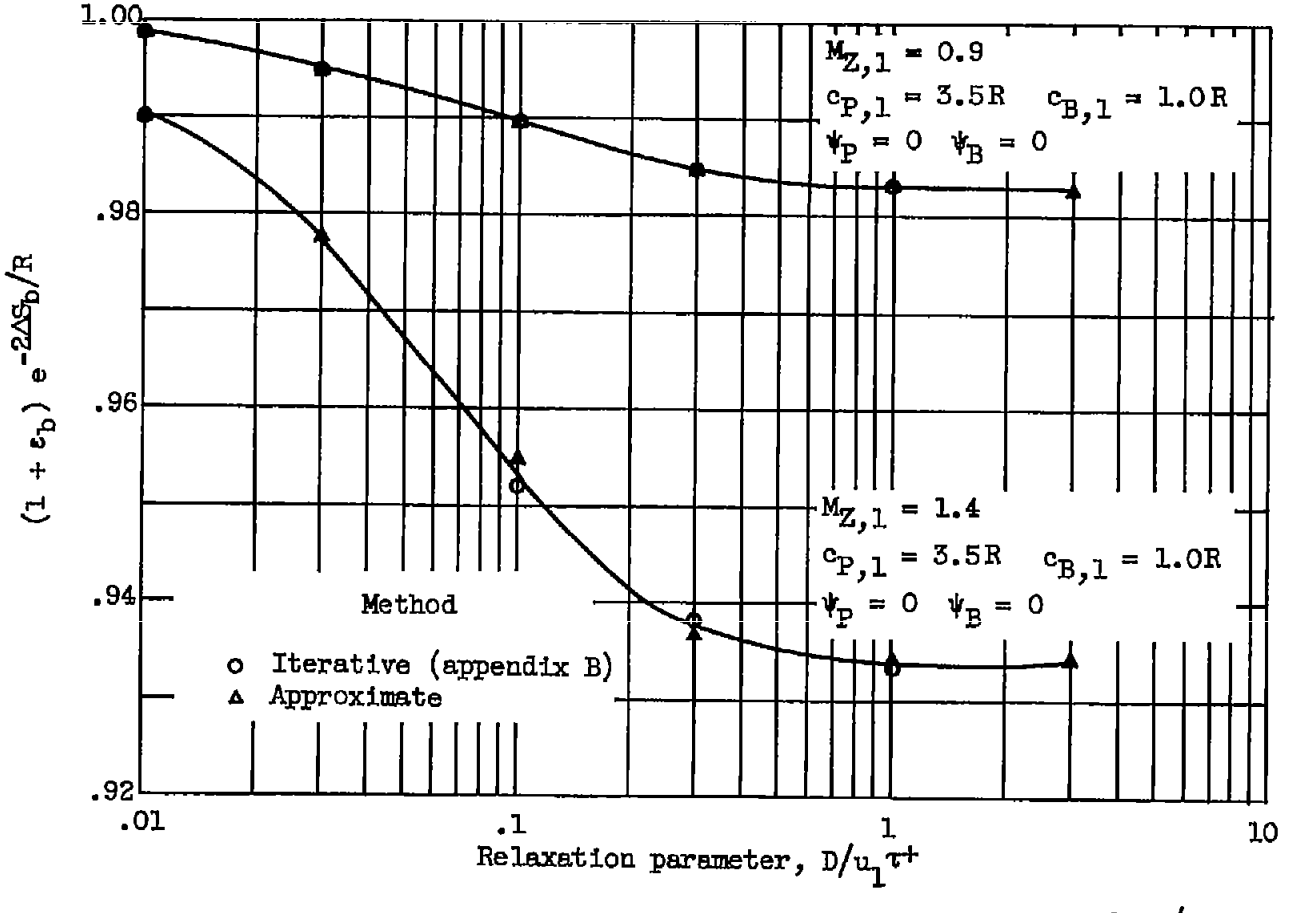


Figure 18. - Comparison of calculations of $(1 + \varepsilon_b)\ e^{-2\Delta S_b/R}$.